Final Report Under
NASA Grant NAG 1-490,
"Analysis of an Angle-Only MLS Guidance System"

ANALYSIS OF A RANGE ESTIMATOR WHICH USES MLS ANGLE MEASUREMENTS

KU-FRL-671-1

Prepared by

David R. Downing

and

Dennis Linse

Flight Research Laboratory
University of Kansas Center for Research, Inc.
Lawrence, Kansas 66045

July 1987

ABSTRACT

A concept that uses the azimuth signal from a microwave landing system (MLS) combined with onboard airspeed and heading data to estimate the horizontal range to the runway threshold is investigated. The absolute range error is evaluated for trajectories typical of general aviation (GA) and commercial airline operations (CAO). These include constant intercept angles for GA and CAO, and complex curved trajectories for CAO. It is found that range errors of 4000-6000 feet at the entry of MLS coverage which then reduce to 1000-foot errors at runway centerline intercept are possible for general aviation operations. For commercial airline operation, errors at entry into MLS coverage of 2000 feet which reduce to 350 feet at runway centerline interception are possible.

ACKNOWLEDGEMENTS

The authors wish to thank Mr. Wayne Bryant, Contract Monitor, NASA Langley Research Center, for his assistance and direction. We would also like to thank Mr. Douglas Niemoller and Mr. Rupert Girouz of Bendix Air Transport Avionics Division for supplying information on their MLS receiver.

TABLE OF CONTENTS

LIST OF FIGURES

LIST OF TABLES

LIST OF SYMBOLS

A_z	Azimuth relative to runway centerline (deg)
$\dot{A}_z$	Azimuth rate (deg/sec)
R	Horizontal range to runway threshold (ft)
t	Time (sec)
V_G	Ground velocity (fps)
V_x, V_y	Velocity perpendicular and parallel to runway centerline (fps)
V_x', V_y'	Velocity perpendicular to and along radial to runway (fps)
$\lvert\Delta\tilde{R}\rvert$	Absolute error in horizontal range (ft)
ε_{A_z}	MLS system azimuth error (deg)
ε_v	Airspeed sensor error (fps)
ε_{v_w}	Wind velocity error (fps)
ε_ψ	Heading gyro error (deg)
ε_{ψ_w}	Wind-related heading error (deg)
ψ_G	Ground track angle (deg)

Notation

$(\ )_n$	Value of ( ) at t_n
$(\tilde{\ })$	Estimated value of ( )
$\Delta(\ )$	Error in ( )

Abbreviations

GA	General Aviation
ILS	Instrument Landing System

MLS	Microwave Landing System
PDME	Precision Distance Measuring Equipment
VOR	Very High Frequency Omin Directional Range

1.0 INTRODUCTION

The FAA, as part of its modernization of the Air Traffic Control System, is replacing the Instrument Landing Systems (ILS) with the Microwave Landing System (MLS). The MLS consists of an angle receiver that gives the vehicle's azimuth and elevation angles relative to the runway centerline, and a precision distance measuring equipment receiver that reads the slant range to the runway centerline. The MLS has several advantages over the ILS, including increased volumetric coverage, e.g. ±30° in azimuth as opposed to ±2.5° for ILS; less susceptibility to interference or multipath problems; and full three-dimensional navigation as opposed to angular deviation from the centerline and fixed glide slope. One advantage of the three-dimensional navigation capability of the MLS is that it permits the implementation, when combined with a CRT display, of a pictorial horizontal situation display.

Although the MLS will provide all the above advantages, its use will require the re-equipping of the nation's fleet of aircraft. One segment for which this will have a particularly severe impact is general aviation (GA) aircraft. The cost of a full set of MLS airborne equipment is estimated to be approximately $4,700. Although this is only about two times the cost of a new ILS receiver, it must be remembered that a significant number of the present GA fleet of approximately 200,000 already have the ILS equipment. Any technique that can reduce the financial impact of

this re-equipping of the GA fleet while providing a system with at least the capability of the current ILS would be welcomed.

This report presents a feasibility study to determine the performance of a system that uses only the MLS angle receiver to estimate the horizontal position of the aircraft relative to the runway threshold. Measurements of the vehicle's azimuth, airspeed, and heading are combined with a derived azimuth rate to estimate the vehicle's horizontal range to the runway threshold. This provides an estimate of the vehicle's horizontal position.

The advantage of this technique, if feasible for a GA aircraft, would be that it would not be necessary to purchase a PDME receiver, which would represent an approximate saving of 50%. In addition, the angle-only MLS algorithm could have an important use as a backup mode for aircraft equipped with the full MLS in the case of a PDME failure. Although, if the PDME failed, it would always be possible to revert to the constant heading centerline intercept technique currently used with the ILS, this would require larger airspace and would reduce the landing efficiency as measured by landing per hour.

The remainder of this report presents the angle-only MLS algorithm, a linear error analysis, and a simulation study.

2.0 ANGLE-ONLY MLS CONCEPT

The MLS angle receiver provides measures of aircraft azimuth and elevation relative to the runway. The concept investigated makes use of the rate of change of the azimuth angle to estimate the aircraft's horizontal position. The basic MLS geometry is shown in Figure 1. The aircraft has ground speed given by V_G and a ground track angle relative to the runway heading given by ψ_G. There are two coordinate frames of interest, the X-Y frame which is aligned parallel and perpendicular to the runway centerline, and the X'-Y' frame which is perpendicular to the radius vector and along the radial vector.

It is possible to express the aircraft velocity in the X-Y axes using measured ψ_G:

$$V_x = V_G \text{ Sin } \psi_G$$
$$V_y = V_G \text{ Cos } \psi_G \tag{1}$$

Then using A_z measured by the MLS angle receiver, the tangential and radial components are given by

$$\begin{bmatrix} V_{x'} \\ V_{y'} \end{bmatrix} = \begin{bmatrix} \text{Cos } A_z & -\text{Sin } A_z \\ \text{Sin } A_z & \text{Cos } A_z \end{bmatrix} \begin{bmatrix} V_x \\ V_y \end{bmatrix} \tag{2}$$

Finally it is recognized that

$$V_{x'} = \dot{A}_z R \tag{3}$$

Therefore the horizontal range, R, can be written

$$R = \frac{V_G}{\dot{A}_z} [\text{Sin } \psi_G \text{ Cos } A_z - \text{Cos } \psi_G \text{ Sin } A_z]$$

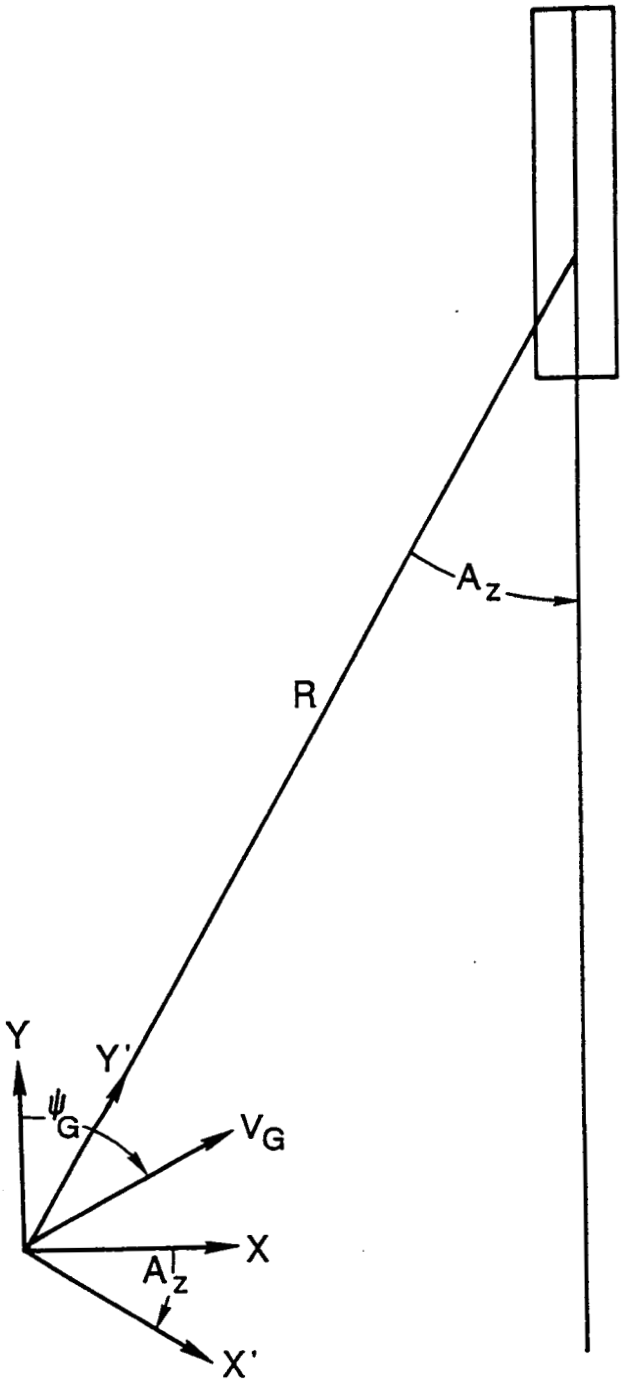

Figure 1: Definition of Problem Geometry

or, using a trigonometric identity, this reduces to

$$R = \frac{V_G}{\dot{A}_z} \text{Sin } (\psi_G - A_z) \tag{4}$$

If $\dot{A}_z$ can be derived from A_z, the aircraft's position in the horizontal plane is determined by R and A_z. This information can then be used as an input to a 3-D guidance system, to drive a horizontal map display, or as part of a landing guidance system.

3.0 LINEAR ERROR ANALYSIS

The angle-only MLS concept is complicated by the fact that airspeed rather than ground speed is normally measured; thus winds will introduce errors. Also, the measurements of airspeed and heading will be corrupted by sensor errors, and the azimuth signal will have errors. Finally, the process of deriving $\dot{A}_z$ from the time history of A_z will introduce errors.

To gain insight into how the error sources and the path geometry impact the horizontal range estimate, a linear error model is formed for Equation 4. The range error ΔR is given by

$$\Delta R = \frac{\partial R}{\partial V_G}\Big|_{Nom} \Delta V_G + \frac{\partial R}{\partial \psi_G}\Big|_{Nom} \Delta \psi_G + \frac{\partial R}{\partial A_z}\Big|_{Nom} \Delta A_z + \frac{\partial R}{\partial \dot{A}_z}\Big|_{Nom} \Delta \dot{A}_z \qquad (5)$$

where:
$$\frac{\partial R}{\partial V_G} = \frac{R}{V_G}$$

$$\frac{\partial R}{\partial \psi} = R \cot(\psi_G - A_z)$$

$$\frac{\partial R}{\partial A_z} = -R \cot(\psi_G - A_z)$$

and
$$\frac{\partial R}{\partial \dot{A}_z} = \frac{R}{\dot{A}_z}$$

A second form of the linear analysis is to look at the percent error in the horizontal range estimate $\Delta R/R$ which is given by

$$\frac{\Delta R}{R} = \frac{1}{V_G}\Big|_{Nom} \Delta V_G + \cot(\psi_G - A_z)\Big|_{Nom} \Delta\psi$$

$$- \cot(\psi_G - A_z)\Big|_{Nom} \Delta A_z - \frac{1}{\dot{A}_z}\Big|_{Nom} \Delta\dot{A}_z \qquad (6)$$

This shows that a percent error in ground speed and azimuth rate relates directly in a percent change in range estimate. Again the influence of $\Delta\psi_G$ and ΔA_z are related through the trigonometric term $\cot(\psi_G - A_z)$.

This would lead to the following conclusion. If the error levels were fixed, the algorithm would operate better as the airspeed increased and as the azimuth rate increased. Also the influence of heading and azimuth errors would decrease if paths were selected that kept $\psi_G - A_z$ close to 90°. This would correspond to constant radius or circular paths about the MLS transmitter.

4.0 SYSTEM SIMULATION

4.1 Introduction

To evaluate the accuracy of the horizontal range predicted by Equation (4) for both general aviation and airliner operation, a batch simulation was developed (Figure 2). The simulation uses a trajectory generator which has a prespecified ground track that the vehicle is constrained to follow. Also the velocity along the path is defined in this routine. This approach does not permit the evaluation of any interaction of nominal trajectory and piloting technique or pilot performance. The output of the trajectory generator is a history of the true vehicle position $\underline{X}_n$ at $t = t_n$. Using the current true position and the runway and MLS geometry, it is possible to calculate the true horizontal range at time t_n, R_n and the true azimuth A_z.

The true measures of velocity, heading, and azimuth are corrupted by sensor errors and errors in the wind magnitude and direction to form the measured values $\tilde{V}_G$, $\tilde{\psi}_G$, and $\tilde{A}_z$. The estimate of azimuth rate, $\dot{\tilde{A}}$, is calculated using the current and past values of the measured azimuth as

$$\dot{\tilde{A}} = \frac{\tilde{A}_{z_n} - \tilde{A}_{z_{n-1}}}{DT} \tag{7}$$

with DT being the algorithm update rate. The approximate values are operated on by the range equation to form the estimated horizontal range $\tilde{R}_n$ as

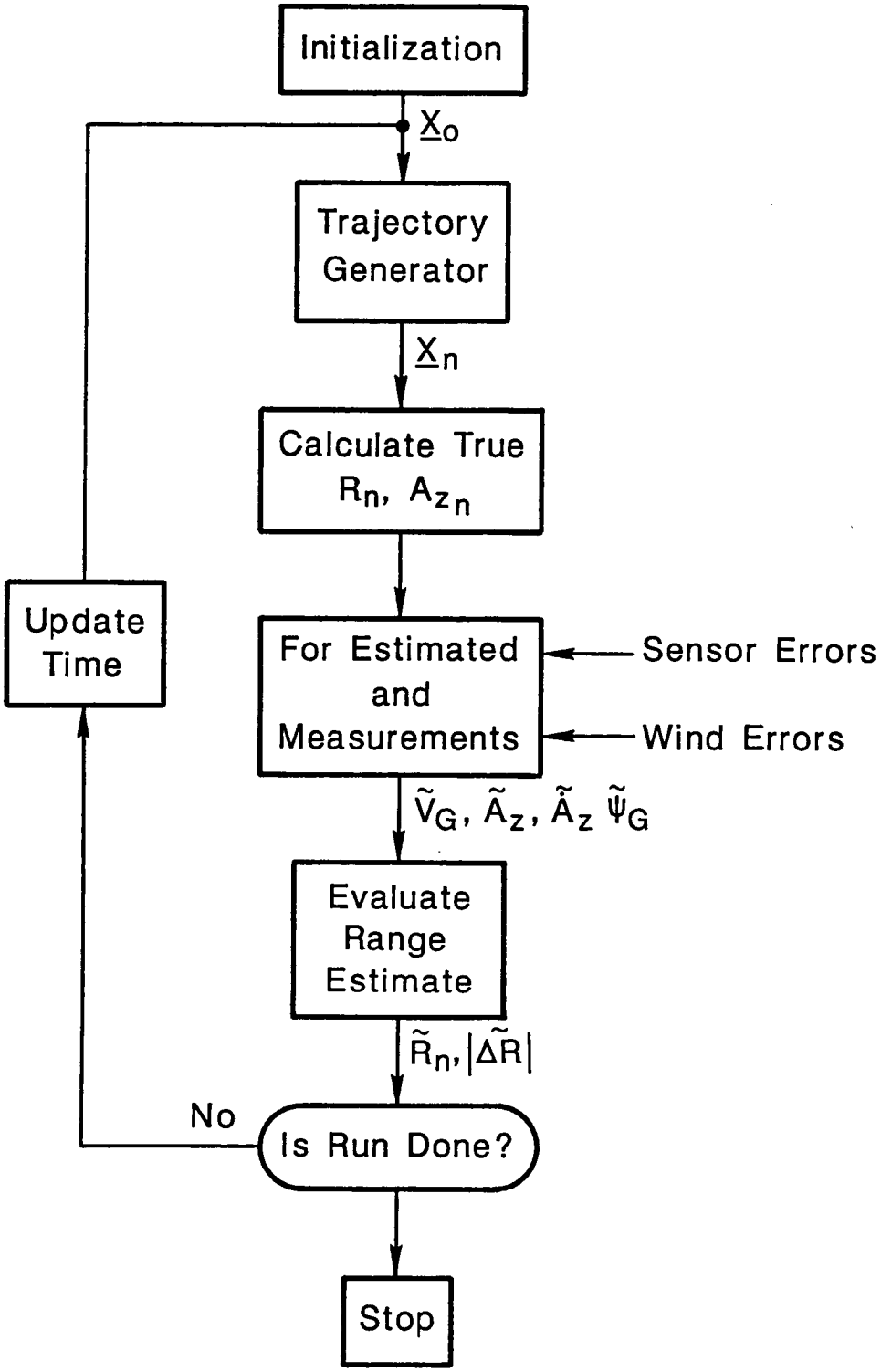

Figure 2: Simulation Block Diagram

$$\tilde{R}_n = \frac{V_{G_n}}{\dot{\tilde{A}}_{z_n}} \sin(\tilde{\psi}_{G_n} - \tilde{A}_{z_n}) \tag{8}$$

$\tilde{R}_n$ is compared with R_n to form the absolute range error, $|\Delta\tilde{R}|$. The time is incremented, and the vehicle is moved to the next point on the nominal trajectory. This continues until the prescribed path is completed. A listing of the simulation program is included in Appendix A.

A detailed discussion of the sensor and wind error models and the nominal trajectories used in the evaluation are discussed in the next section.

4.2 Error Models

The error sources evaluated for general aviation operation included azimuth errors, airspeed sensor errors, heading gyro errors, azimuth receiver errors, and wind direction and magnitude errors. For airliner operation, the errors include azimuth errors, ground speed errors, and ground track errors.

To determine the effect of wind errors for GA cases, it is assumed that at the start of the approach an estimate of the runway winds would be provided. This would most likely be sent to the vehicle from the ground. This wind data (speed and heading) would be input into the range algorithm and would also be used to set up a crab angle so that the vehicle could fly the desired ground track. If either or both the speed and heading were in error, there would

be an effective error in the speed and the heading used in the range calculation. The effect of these errors will depend on the nominal wind direction and the flight path. For this study, nominal winds of 20 fps from ±45 degrees from the centerline were chosen as representative. Wind errors of 5 fps in speed and 5 degrees in direction were then introduced into the calculations.

The analysis assumed all errors were deterministic and of an additive nature. The ground speed model was

$$\tilde{V}_G = V_G + \varepsilon_v + \varepsilon_{v_w} \tag{9}$$

where

$\tilde{V}_G$ is the estimated ground speed

V_G is the true ground speed

ε_v is the airspeed sensor error

ε_{v_w} is the wind velocity error

The vehicle heading model was

$$\tilde{\psi}_G = \psi_G + \varepsilon_\psi + \varepsilon_{\psi_w} \tag{10}$$

where

$\tilde{\psi}_G$ is the estimated ground track

ψ_G is the true ground track

ε_ψ is the error in heading gyro

ε_{ψ_w} is the error in heading due to an error in wind.

The azimuth model was

$$\tilde{A}_z = A_{z_T} - \varepsilon_{A_z} \tag{11}$$

where

$\tilde{A}_z$ is the measured azimuth

A_{z_T} is the true azimuth

ε_{A_z} is the MLS azimuth system error (transmitter and receiver)

With a constant bias model assumed in this study for ε_{A_z} there will be no effective error in the azimuth rate, since

$$\tilde{\dot{A}}_z = \frac{\tilde{A}_{z_n} - \tilde{A}_{z_{n-1}}}{DT} = \frac{A_{z_{T_n}} - A_{z_{T_{n-1}}}}{DT} \tag{12}$$

The only error introduced in $\tilde{\dot{A}}_z$ is due to the discrete approximation of the derivative. This error was found to be very small (i.e., less than 80 ft) when compared with the other sensor and wind errors.

Table 1 presents the detailed values used for the error sources. This consists of two cases: the first covers a range of values representative of general aviation instruments, and the second uses error magnitudes representative of the sensors available on commercial ailiners.

4.3 Nominal Trajectories

Two classes of nominal trajectories were evaluated. The first class, Figure 3, is similar to current ILS practices in that constant intercept legs are flown to near the runway centerline. In this study, four nominal trajectories were evaluated with combination of two intercept angles, 30° and 45°, and two intercept ranges, 12,500 feet and 25,000 feet. The second class of trajectories was selected as representative of future complex trajectories, Figures 4a and 4b, that would be used to improve runway efficiency. In the research discussed in References 1 and 2, these trajectories were flown using the full MLS angle and Precision Distance Measuring Equipment range measurements.

Table 2 identifies the velocities and nominal trajectories evaluated.

Table 1: Sensor Errors

Error Values	General Aviation Instruments	Airliner Instruments
Airspeed	1, 5, and 10 fps	*
Heading	1, 2, 5 deg	.5 deg
Ground Speed	Not available	1.5 fps
MLS Azimuth	.32 deg	.32 deg

*Airspeed not used if groundspeed available.

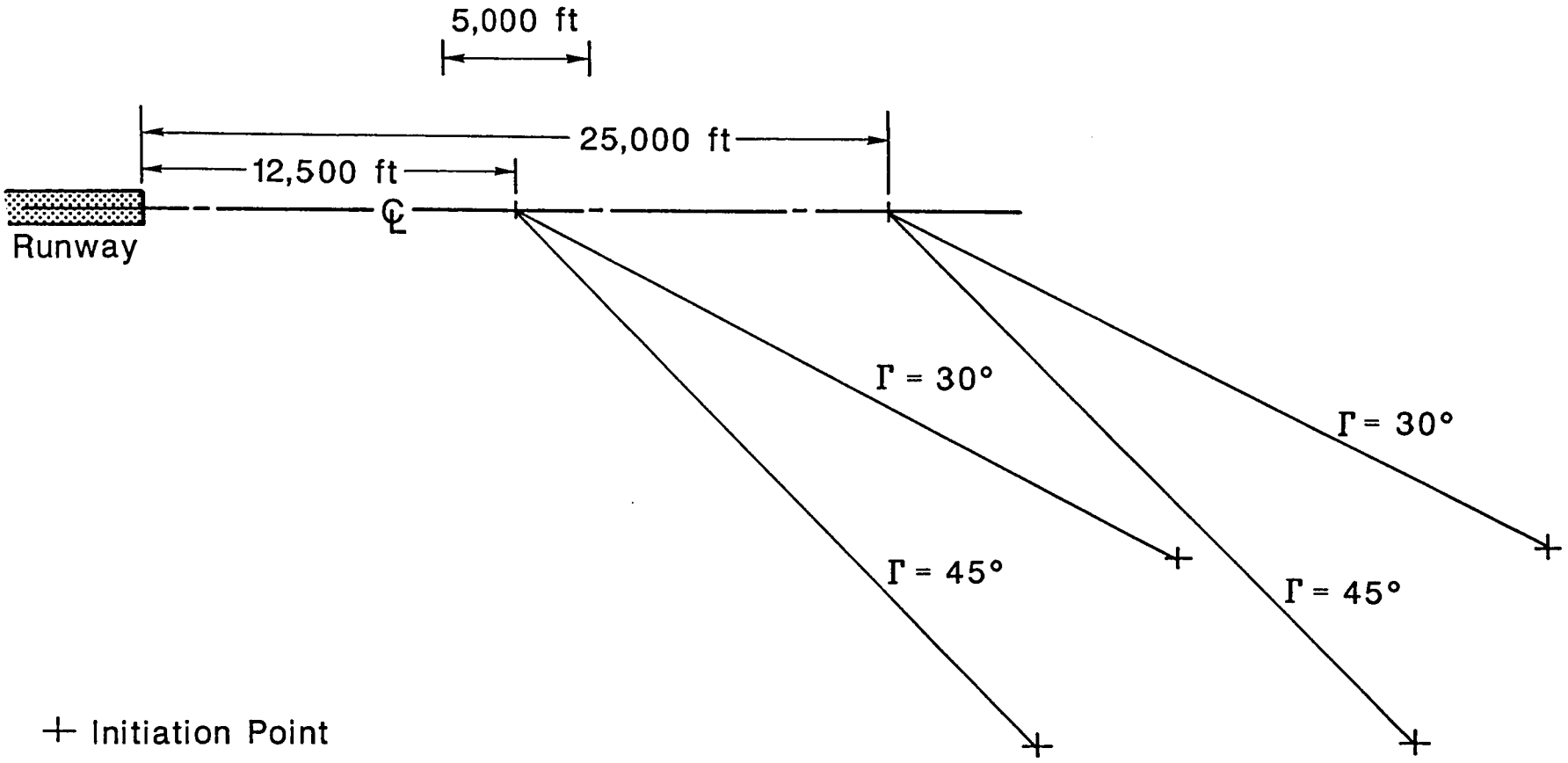

Figure 3: Constant Intercept Angle Nominal Trajectories

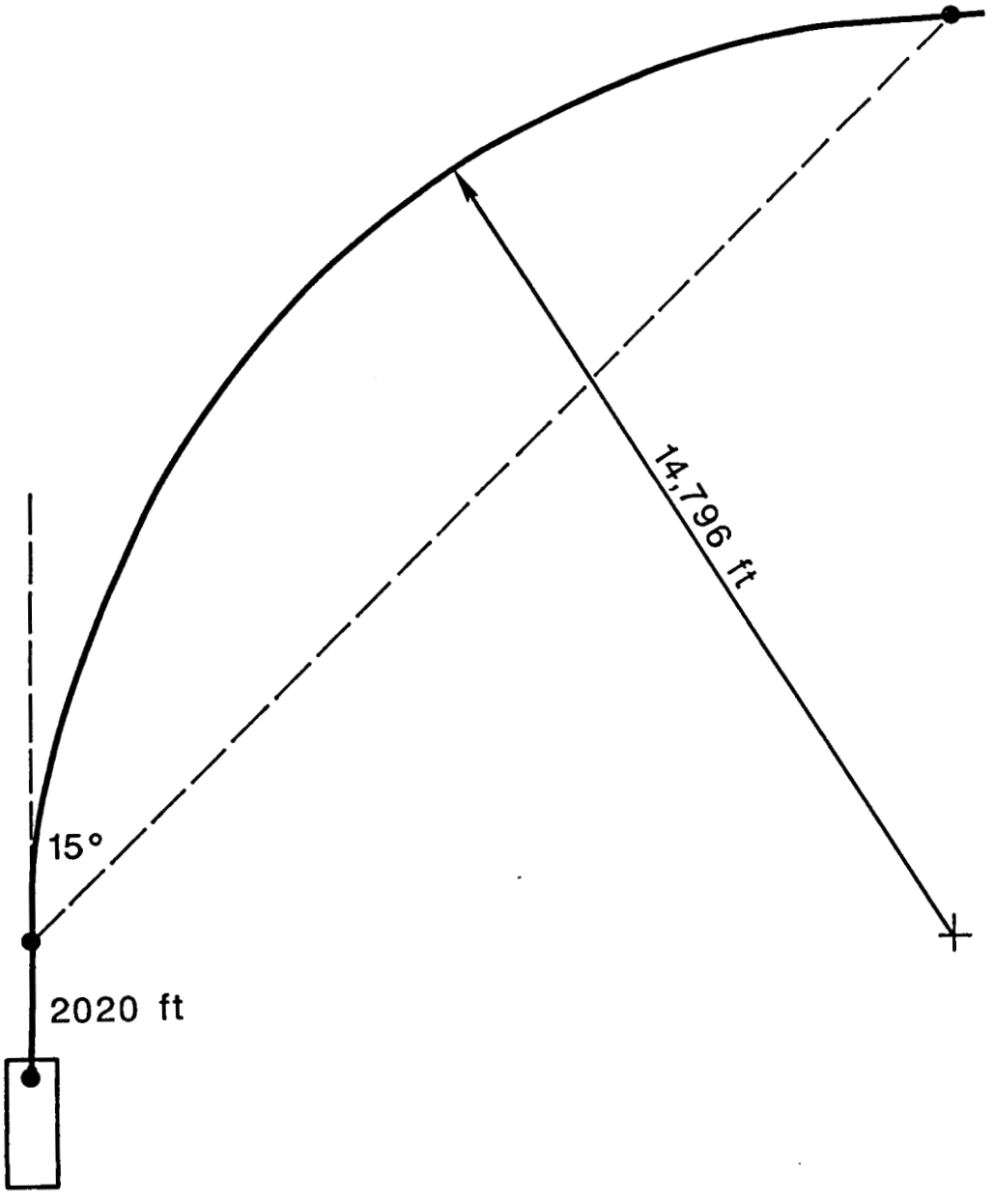

Figure 4a: Complex Trajectory 1

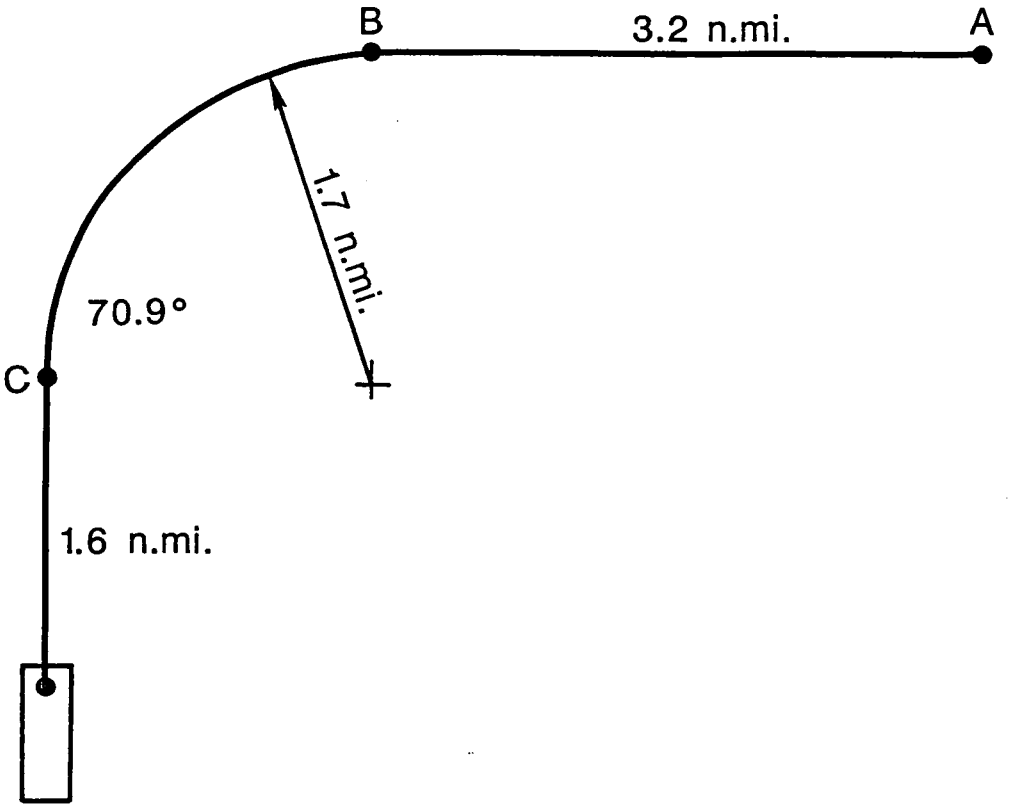

Figure 4b: Complex Trajectory 2

Table 2: Nominal Test Trajectories

Class 1 Trajectories:

Airspeed	Intercept Angle	Intercept Range
160 fps	30° and 45°	12,500 and 25,000 ft
236 fps	30° and 45°	12,500 and 25,000 ft

Class 2 Trajectories:

Airspeed	Trajectory
236 fps	1 and 2

5.0 SIMULATION RESULTS

The results of the simulation will be divided into the two classes, GA and commercial airline operations. For each class, representative plots of absolute estimated range error versus range are presented for both individual error sources and combinations of errors. Care should be exercised in interpreting the results for simultaneous error sources. The errors, as calculated, are not additive, and some multiple error cases may show values for estimated range error smaller than those shown for individual errors. A complete set of simulation runs is included in Appendix B.

5.1 Performance Typical of General Aviation Operation

The general aviation cases are flown at 160 fps. Plots of absolute range error, $|\Delta\tilde{R}|$, versus range for the case of a 45° intercept at 12,500 feet are given in Figures 5a and 5f. These curves are representative of all the cases investigated. The estimated range error $\Delta\tilde{R}$ due to the estimate of $\dot{A}_z$ is not shown because of its relative small value. For all GA cases the error was always less than 40 feet. From Figure 5 it can be seen that $|\Delta\tilde{R}|$ have their maximum values at the start of the run and decrease as the runway centerline is approached. Figure 5c shows that an error in heading is the dominant error source. (Figure 5a shows that while of small value, airspeed errors are also

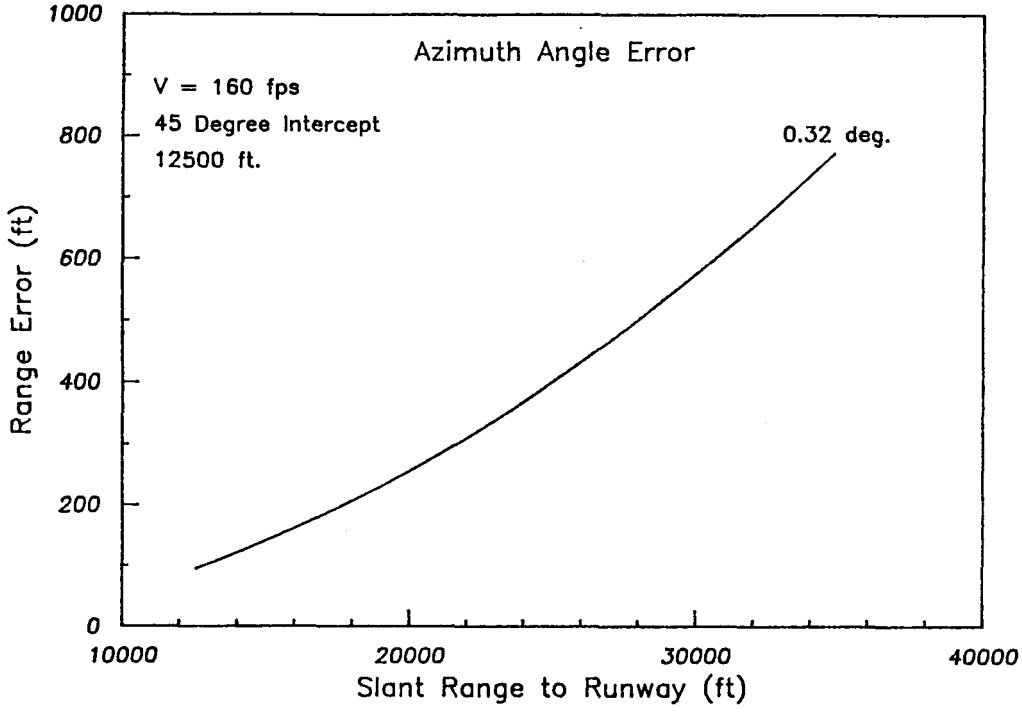

Figure 5a: Range Estimation Error Due to Azimuth Angle Error for Constant Intercept Trajectory

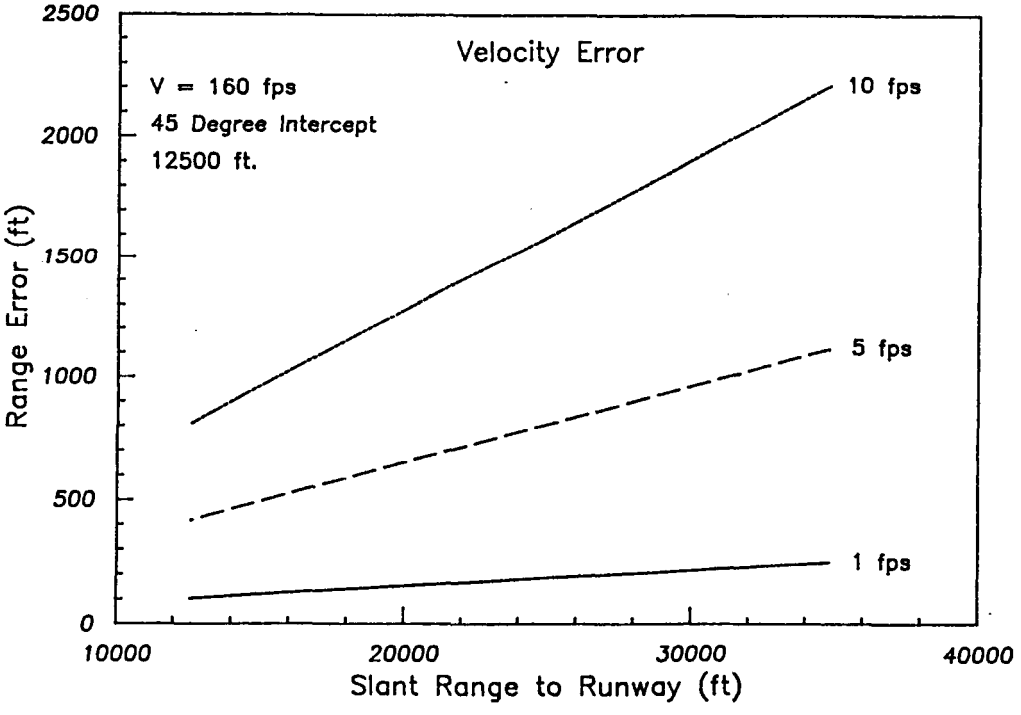

Figure 5b: Range Estimation Error Due to Airspeed Sensor Errors

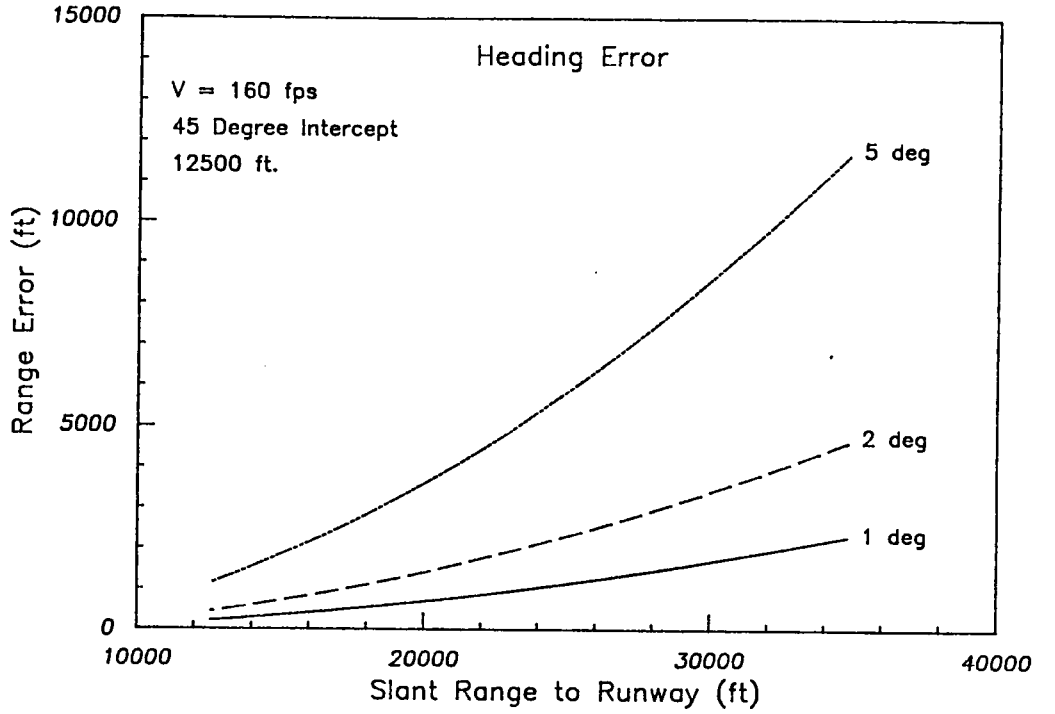

Figure 5c: Range Estimation Error Due to Heading Sensor Error

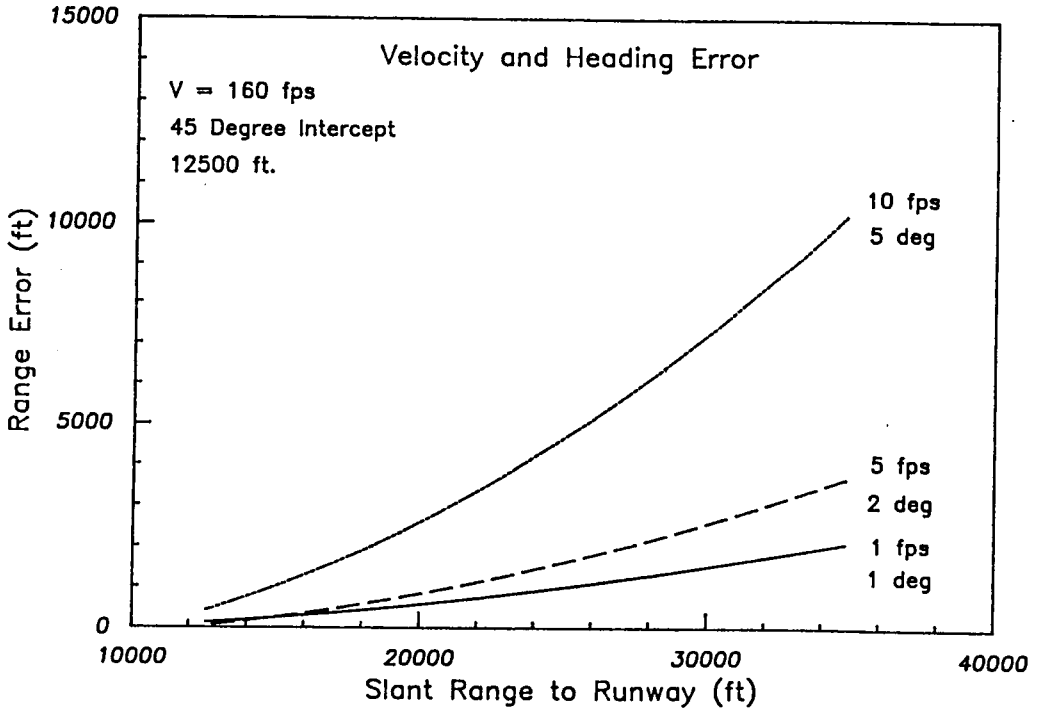

Figure 5d: Range Estimation Error Due to Airspeed and Heading Sensor Errors

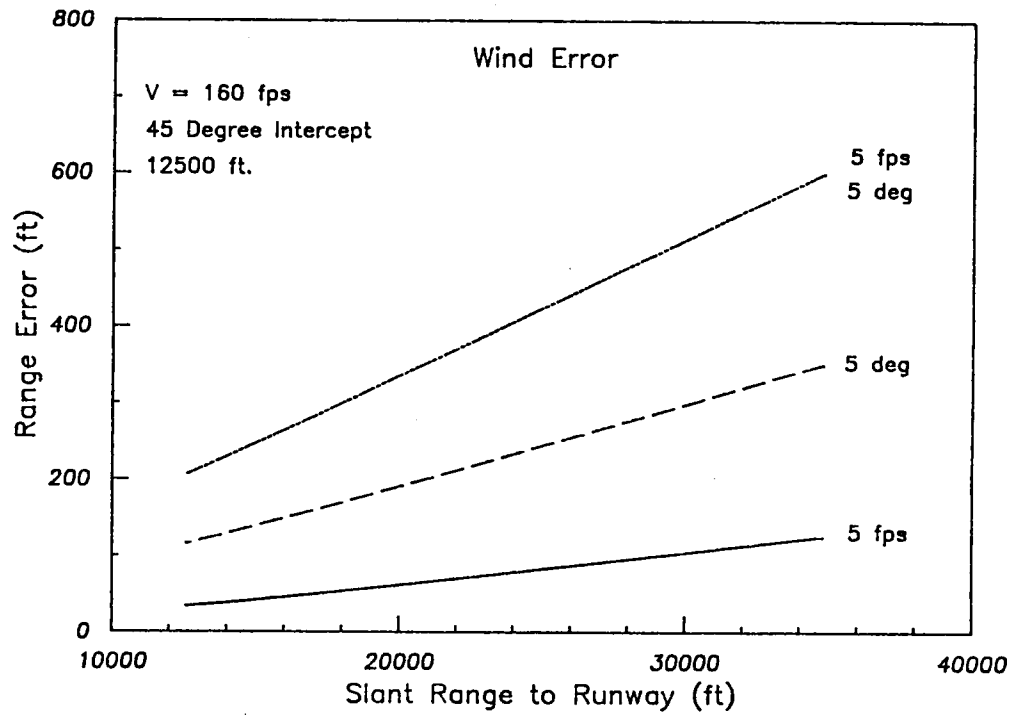

Figure 5e: Range Estimation Error Due to Uncertainties in Wind Information. Nominal Wind: 20 fps from 135 deg.

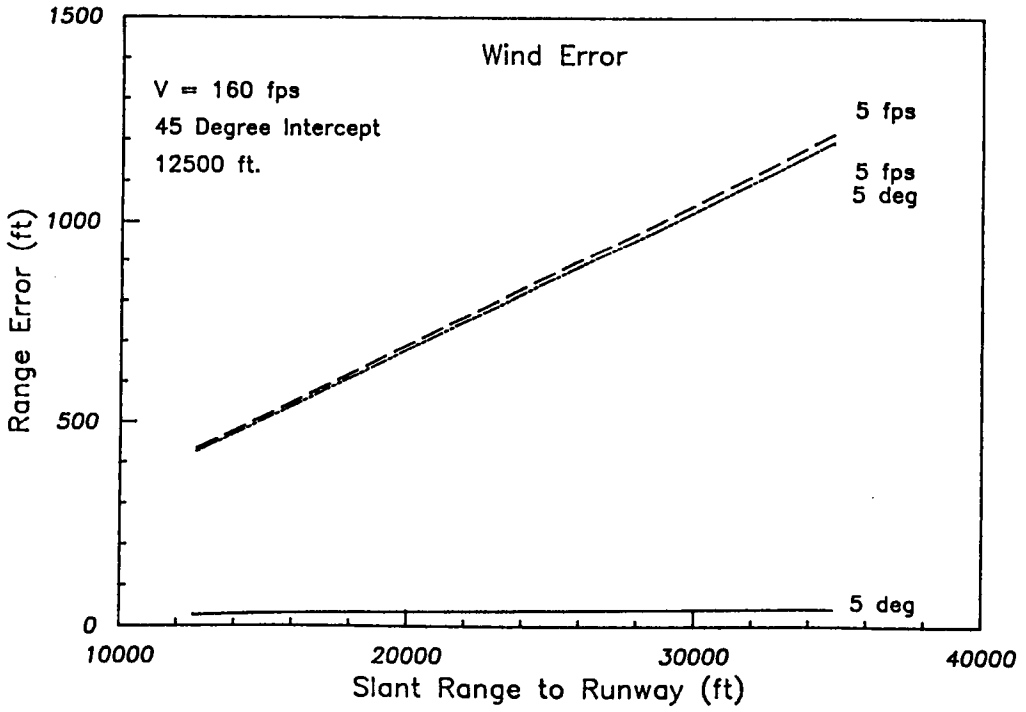

Figure 5f: Range Estimation Error Due to Uncertainties in Wind Information. Nominal Wind: 20 fps from 225 deg.

significant. MLS azimuth errors are relatively insignificant.) An interesting behavior is shown in Figures 5e and 5f which present the effects of errors in the knowledge of the winds. It is seen that $|\tilde{\Delta R}|$ depends on the nominal wind direction.

$|\tilde{\Delta R}|$ is approximately twice as large if the nominal wind is from 225° (crosswind) as opposed to from 135° (headwind). This could be due to the fact that with a headwind, $\dot{A}_z$ will be slower than predicted while ΔV_A will be higher. These errors will tend to cancel as shown by Equation (6). When the wind error is a crosswind error, these effects do not cancel.

Tables 3a and 3b summarize the total simulation runs by presenting the initial and final value of $|\tilde{\Delta R}|$. They show the same dominance of heading errors. Also shown in Tables 3a and 3b are the effects of intercept angle and intercept range. For a fixed intercept range you get larger values of $\tilde{AR}$ throughout the mission using a 30° intercept angle rather than a 45° intercept angle. This is true for both 12,500 and 25,000 feet intercept range.

The better intercept range is not as clear, since no overall consistent pattern is seen. It can be seen, however, that the value of $|\tilde{\Delta R}|$ at centerline intercept is smaller for the 12,500 ft intercept than for the 25,000 ft intercept. Both of these effects, i.e. the small errors for 45° and 12,500 ft intercept, are believed due to the higher range of $\dot{A}_z$.

Table 3a: Range Error Summary for General Aviation;

V = 160 fps, Intercept at 25,000 ft

Error Case					45° Intercept		30° Intercept	
ε_{A_z} (deg)	ε_V (fps)	ε_ψ (deg)	ε_{V_w} (fps)	ε_{ψ_w} (deg)	Initial Error (ft)	Error at Intercept (ft)	Initial Error (ft)	Error at Intercept (ft)
.32	0	0	0	0	648	163	1031	272
0	1	0	0	0	318	180	332	185
0	5	0	0	0	1470	807	1536	813
0	10	0	0	0	2909	1591	3042	1598
0	0	1	0	0	1911	422	3103	739
0	0	2	0	0	3866	874	6251	1513
0	0	5	0	0	9804	2273	15,768	3878
0	1	1	0	0	1636	268	2822	587
0	5	2	0	0	2548	117	4942	776
0	10	5	0	0	7539	848	13,745	2552
0	0	0	5	0	177	90	584	293
0	0	0	0	5	474	252	473	235
0	0	0	5	5	805	432	1205	617
0	0	0	5	0	1620	876	1644	846
0	0	0	0	5	48	32	185	107
0	0	0	5	5	1594	862	1453	747

Note: * Nominal wind 20 ft/sec from 135 deg

** Nominal wind 20 ft/sec from 225 deg

Table 3b: Range Error Summary for General Aviation;

V = 160 ft/sec, Intercept at 12,500 ft

Error Case					45° Intercept		30° Intercept	
ε_{A_z} (deg)	ε_v (fps)	ε_ψ (deg)	ε_{v_w} (fps)	ε_{ψ_w} (deg)	Initial Error (ft)	Error at Intercept (ft)	Initial Error (ft)	Error at Intercept (ft)
.32	0	0	0	0	772	94	1186	151
0	1	0	0	0	248	102	258	107
0	5	0	0	0	1120	417	1164	422
0	10	0	0	0	2209	810	2297	817
0	0	1	0	0	2292	202	3283	359
0	0	2	0	0	4625	430	7208	750
0	0	5	0	0	11,675	1136	18,130	1943
0	1	1	0	0	2089	124	3379	283
0	5	2	0	0	3681	50	6302	380
0	10	5	0	0	10,229	421	17,001	1278
0	0	0	5	0	126	34	431	134
0	0	0	0	5	350	115	347	105
0	0	0	5	5	601	206	899	297
0	0	0	5	0	1219	430	1230	413
0	0	0	0	5	43	26	147	66
0	0	0	5	5	1199	423	1086	363

Note: * Nominal wind 20 ft/sec from 135 deg.

** Nominal wind 20 ft/sec from 225 deg.

5.2 Performance Typical for Commercial Airline Operations

The error in estimate range, $|\Delta\tilde{R}|$, was evaluated for commercial airline operations at a velocity of 236 ft/sec. Two types of nominal trajectory were flown: (1) the same constant intercept angles trajectories used in the GA runs and (2) two special complex trajectories designed to better utilize the large azimuth coverage offered by the MLS system.

5.2.1 Constant Intercept Angle Trajectories

A plot of the estimated range error, $|\Delta\tilde{R}|$, versus range is shown in Figure 6 for the case of 45° intercept angle at 25,000 feet intercept range. As with the GA runs, the range error decreases as the runway centerline is approached. The error throughout the trajectory is significantly better than the GA runs due primarily to the improved instrumentation. As predicted from the linear error analysis, the increase in speed, 236 ft/sec as opposed to 160 ft/sec, will also help in achieving a small error. There are no wind errors evaluated, since the commercial airliner has an inertial navigation system among its sensor complements and can calculate ground speed and ground track angle Γ directly. The dominant single error is the 0.5° error in track angle. The MLS azimuth error is also significant. Table 4 summarizes the four runs made for various

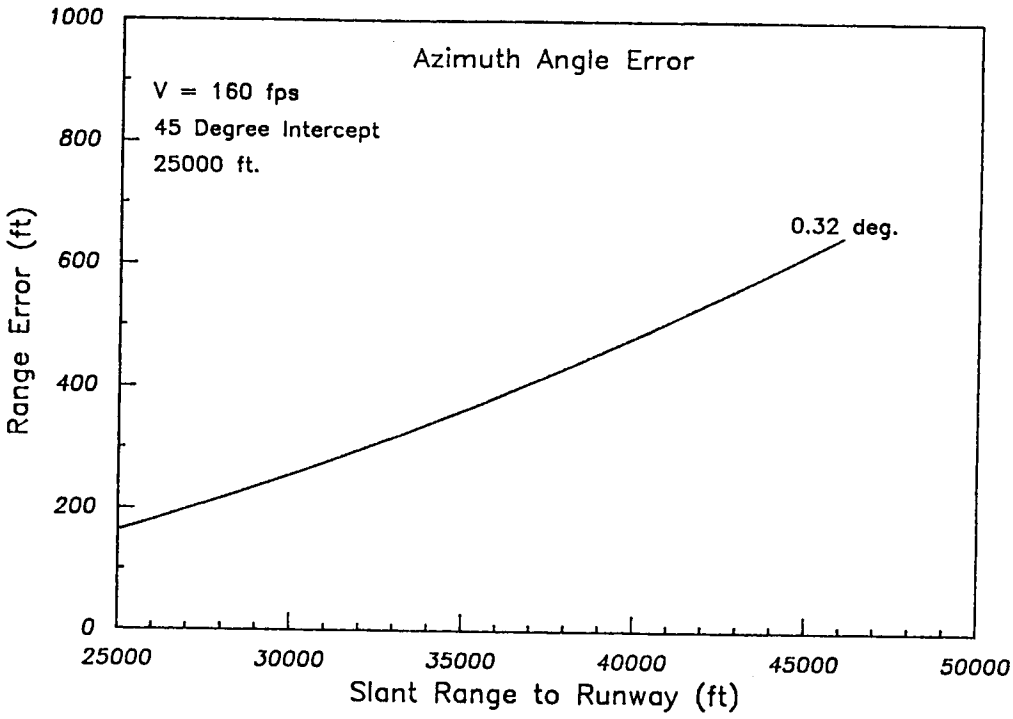

Figure 6a: Range Estimation Error Due to Azimuth Angle Error for Constant Intercept Trajectory

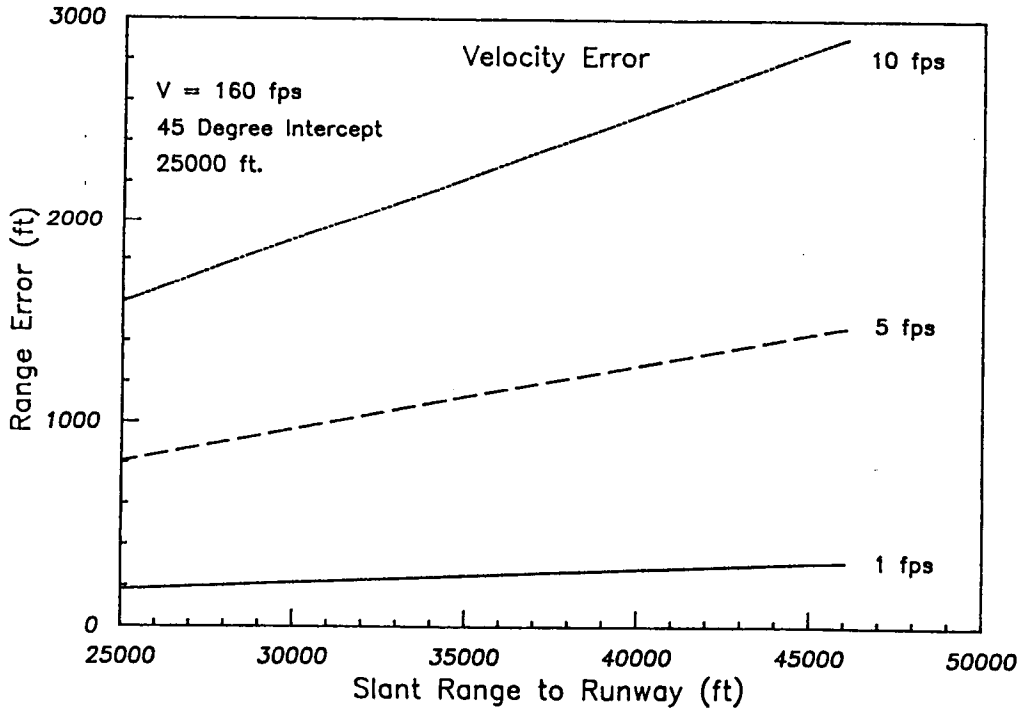

Figure 6b: Range Estimation Error Due to Airspeed Sensor Errors

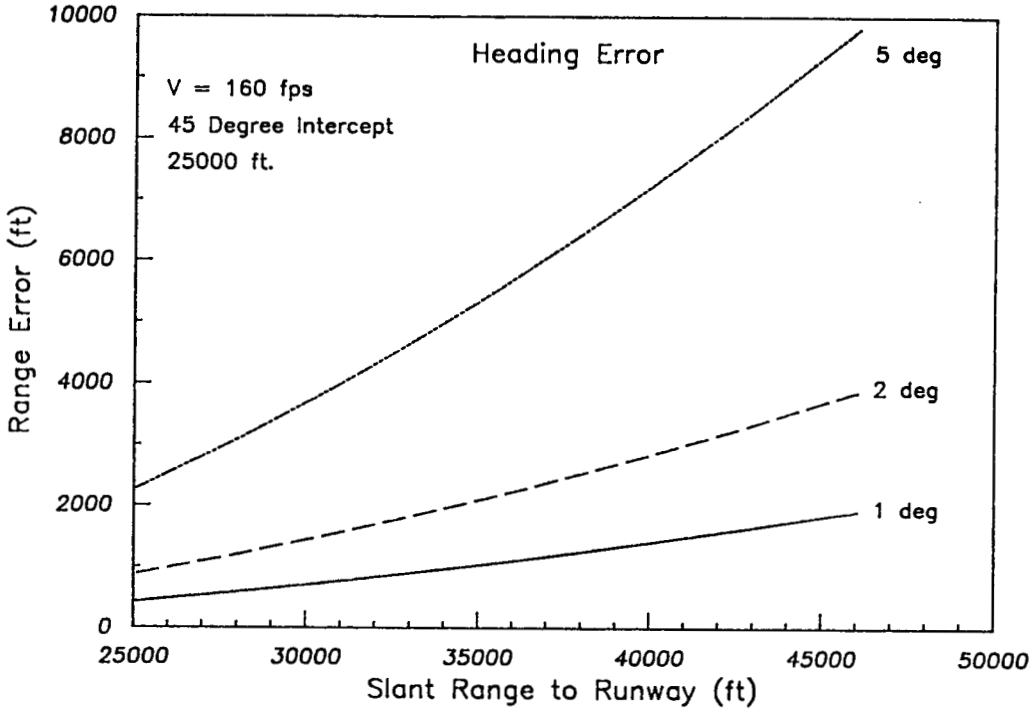

Figure 6c: Range Estimation Error Due to Heading Sensor Error

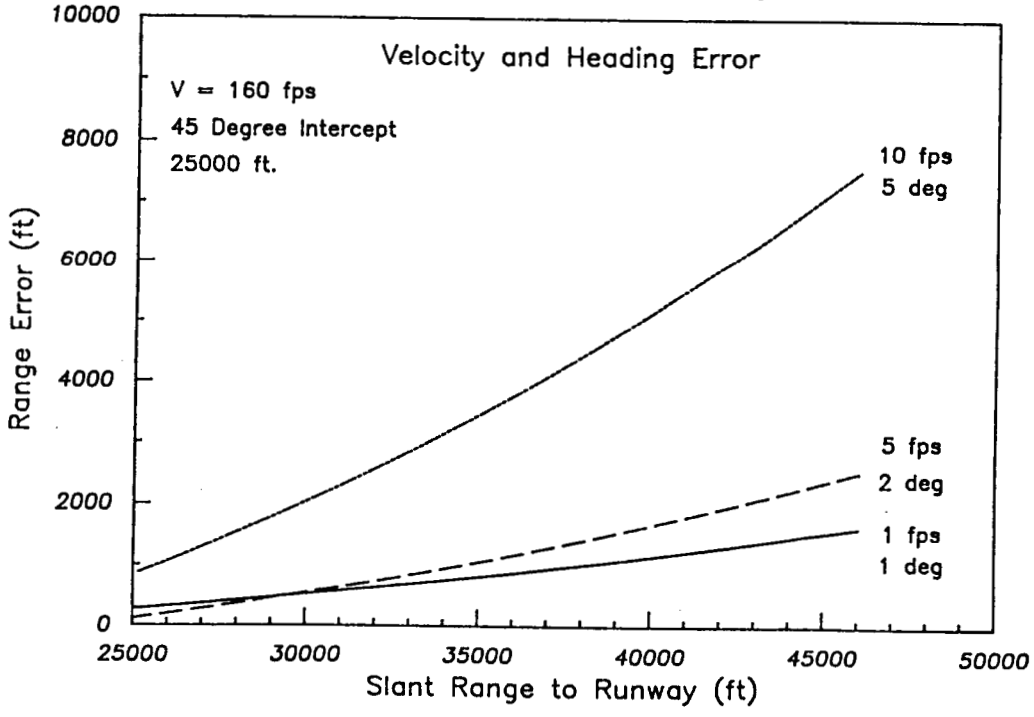

Figure 6d: Range Estimation Error Due to Airspeed and Heading Sensor Errors

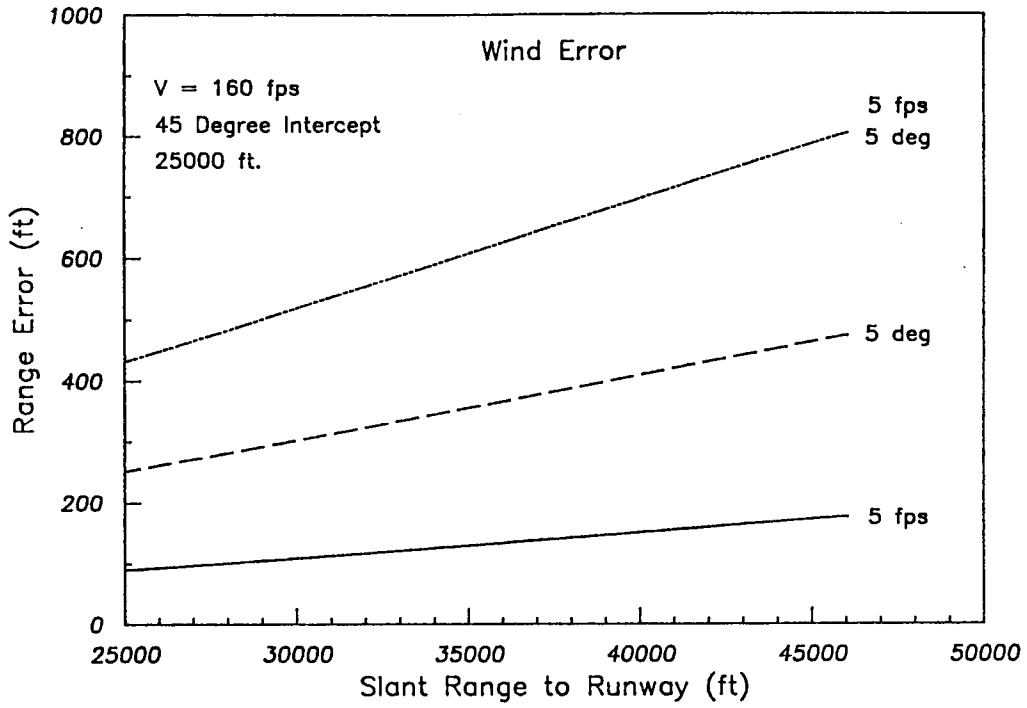

Rigure 6e: Range Estimation Error Due to Uncertainties in Wind Information. Nominal Wind: 20 fps from 135 deg.

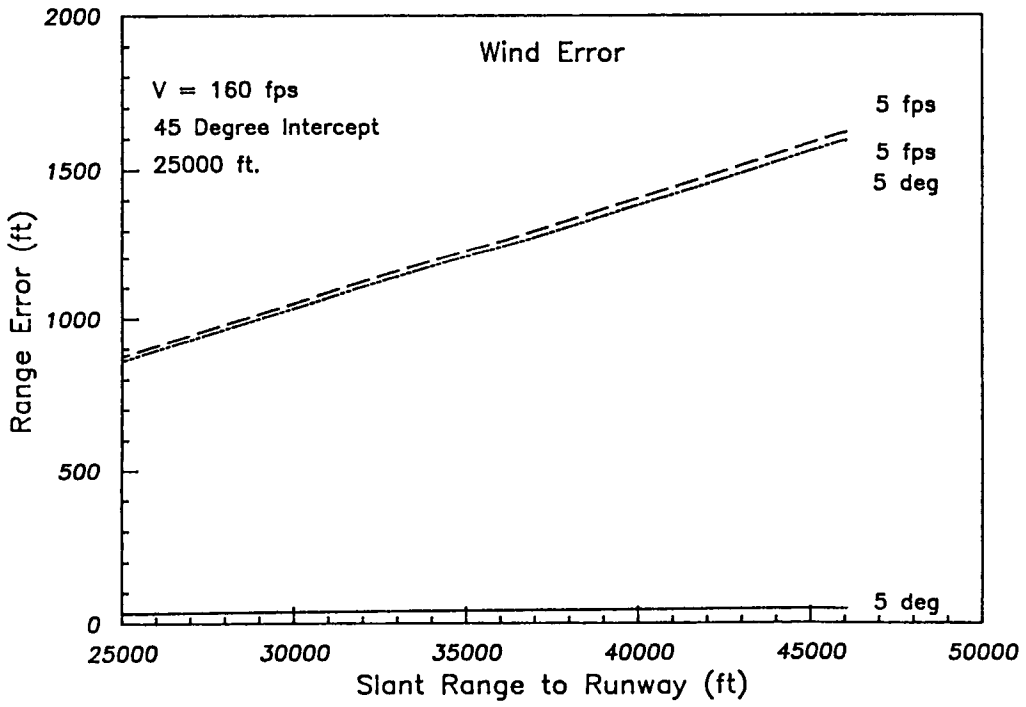

Figure 6f: Range Estimation Error Due to Uncertainties in Wind Information. Nominal Wind: 20 fps from 225 deg.

Table 4: Range Error Summary for Commercial Airliner; V = 236 fps

Error Cases			45° Intercept at 12,500 ft		30° Intercept at 12,500 ft		45° Intercept at 25,000 ft		30° Intercept at 25,000 ft	
ϵ_{A_z} (deg)	ϵ_{V_G} (fps)	ϵ_{Γ} (deg)	Initial Error (ft)	Error at Intercept (ft)	Initial Error (ft)	Error at Intercept (ft)	Initial Error (ft)	Error at Intercept (ft)	Initial Error (ft)	Error at Intercept (ft)
.32	0	0	783	106	1197	166	660	175	1043	286
0	1.5	0	175	47	183	40	249	126	260	119
0	0	.5	1110	79	1753	154	922	189	1515	344
0	1.5	.5	1324	159	1971	233	1209	348	1811	501

intercept angles and ranges. It can be seen that for a fixed intercept range the 45° intercept angle gives smaller error. This again is due to the higher $\dot{A}_z$.

5.2.2 Complex Curved Trajectories

Path 1 (Figure 4a) is a constant radius turn intercepting the runway centerline at 2020 ft. Figure 7 presents the estimated range error. The behavior of the error is different from the constant intercept angle case in that $|\Delta\tilde{R}|$ remains approximately constant from the initial point to a range of approximately 5000 ft. At this point the range error grows rapidly. This rapid growth is due to the fact that the trajectory is tangential to the centerline and thus near the end of the trajectory. $\dot{A}_z$ becomes very small. For ranges greater than 5000 ft the magnitude of the error is relatively small with track angle again being the dominant error.

Path 2 (Figure 4a) exhibits a unique error behavior also (Figure 8) on the initial portion (points A-B). The errors decrease as the centerline is approached with error magnitudes of only a few hundred feet. This good performance is due to the fact that along this portion of the trajectory the aircraft is flying perpendicular to the runway centerline so that $\dot{A}_z$ is almost the maximum possible. From point B to point C, however, the aircraft performs a turn so that its path becomes tangential to the runway centerline. As with path 1, this type of maneuver will lead to small $\dot{A}_z$ and a growing estimate range error.

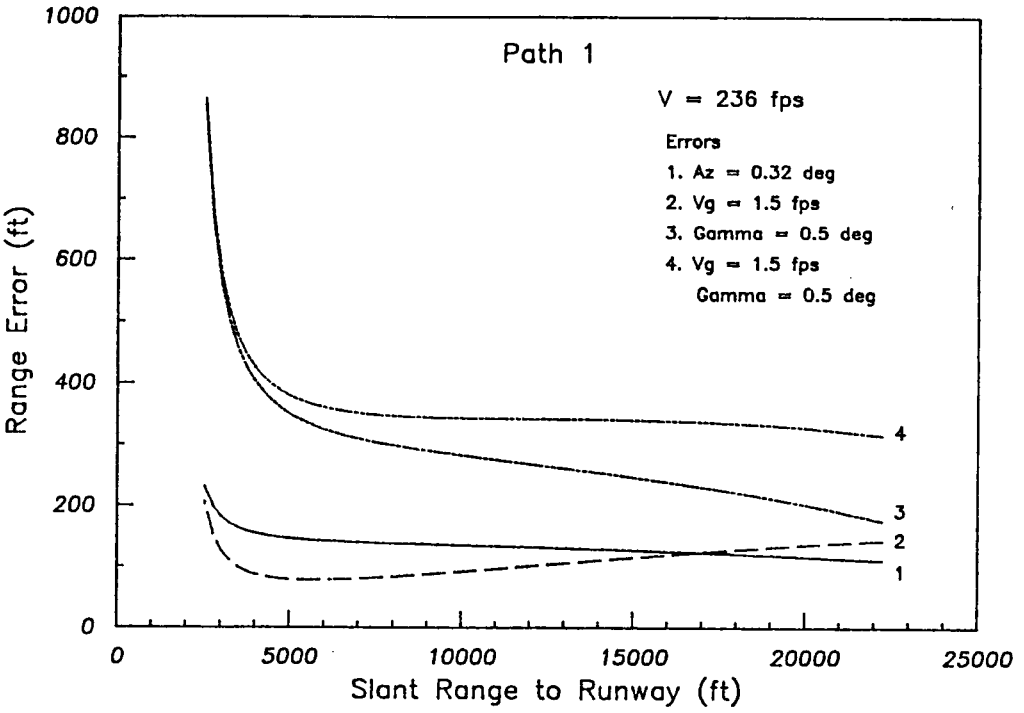

Figure 7: Range Estimation Error for V = 236 fps, Path 1

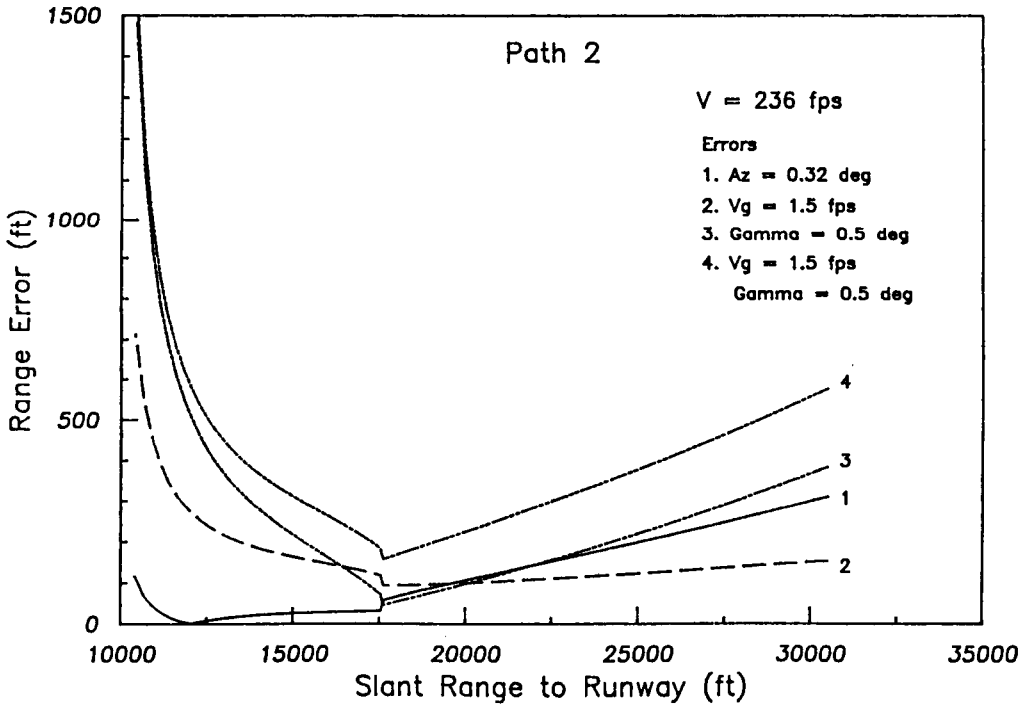

Figure 8: Range Estimation Error for V = 236 fps, Path 2

6.0 CONCLUSIONS AND RECOMMENDATIONS

Based upon the preliminary simulation runs conducted in this study, the following general conclusions can be drawn:

1. To be useful for standard general aviation operation, initial range errors of 4000-6000 ft and errors at runway centerline intercept of 1000 feet must be tolerable. If this were true, a system with a heading error of 2° and an airspeed of 5 ft/sec could achieve this level of performance using the 45° intercept trajectory.
2. To be useful for commercial operation, 2000-foot initial errors and 350-foot errors at the runway centerline intercept must be tolerable. This also could be achieved using the 45° intercept trajectory. Although this may no be acceptable for standard operation, it certainly would be useful as an emergency backup made in case the range signal was lost, or at smaller airports which only have the MLS angle signals. Improved performance is possible by carefully shaping the trajectory. In this case, errors of less than 500 feet are feasible.

In addition to these conclusions, a set of recommendations for future work can be made:

1. It would be useful to investigate the acceptability of this range information by conducting a piloted simulation study. It would also be useful in this study to evaluate methods of providing the pilot with estimates of the

accuracy of the position data: e.g., the estimated position could be shown as the center of a circle that indicates the 50% probability of position.

2. Investigate the combination of the MLS data with other navigation data: e.g., VOR data, to improve the estimates of position. This would be particularly valuable in bounding errors near the centerline when $\dot{A}_z$ approaches zero.

REFERENCES

1. White, William F., and Leonard V. Clark, FLIGHT PERFORMANCE OF THE TCV B-737 AIRPLANE AT KENNEDY AIRPORT USING TRSB/MLS GUIDANCE, NASA TM 80148, July 1979.

2. White, William F., and Leonard V. Clark, FLIGHT PERFORMANCE OF THE TCV B-737 AIRPLANE AT JORGE NEWBERRY AIRPORT, BUENOS AIRES, ARGENTINA, USING TRSB/MLS GUIDANCE, NASA TM 80223, January 1980.

APPENDIX A

This appendix contains the computer program listings used in the simulation studies. The programs are written in Fortran 77 and are organized in the following sections:

Section A.6 presents an example input file (pg. A.19), and Section A.7 presents an example output file (pg. A.20).

A.1 Executive File for Simulation Program

```
      PROGRAM MLSTEST
C
      INTEGER I, PITER, PITER1
C
      CHARACTER RESP*1, FILENAME*14
C
      REAL SO, GAMMA, T, VAIR, VWIND, DWIND, TSAMPLE,
     &     TPRINT, UVAIR, UVWIND, UDWIND, UGAMMA, UAZ, UTSAMPLE
C
      REAL S, VGND, PSI, R, REST, UVGND, RAD, PI, INTANG,
     &     SIGMAR, AZ, AZOLD, AZDOT, RTOVG, RTOGAM, RTOAZ,
     &     RTOAZDOT, DELTAR, X, Y, XOLD, YOLD, VGEST, GAMEST,
     &     A, E, K, P, YO, XOFFSET, YOFFSET, INITGAM, AZEST
C
      LOGICAL FTIME, SCREEN, SPATH
C
      COMMON /DATA/ SO, GAMMA, T, VAIR, VWIND, DWIND, TSAMPLE,
     &              TPRINT, UVAIR, UVWIND, UDWIND, UGAMMA,
     &              UAZ, UTSAMPLE
C
      COMMON /ANALYSIS/ RTOVG, RTOGAM, RTOAZ, RTOAZDOT, SIGMAR
C
      COMMON /COURSE/ A(6), E(6), K, P, YO
C
      WRITE(*,10)
   10 FORMAT(/,' Enter the name of the input data file :')
      READ(*,20) FILENAME
   20 FORMAT(A14)
C
      OPEN(15,FILE=FILENAME)
      OPEN(16,FILE='MLSOUT1.DAT')
      OPEN(17,FILE='MLSOUT2.DAT')
      OPEN(18,FILE='MLSOUT3.DAT')
C
      RAD = 57.29578
      PI  = 3.14159265
      SPATH = .FALSE.
C
C
C   READ IN TH FIXED DATA
C
      CALL READIN (XOFFSET, YOFFSET, SPATH)
      INITGAM = GAMMA
C
   1  CONTINUE
C
C   CORRECT THE INPUT DATA
C
      CALL CORRECT(INITGAM)
C
      WRITE(*,45)
      WRITE(*,40)
```

```
   40 FORMAT(' Do you want a Screen print out? <N> ')
      READ (*,45) RESP
   45 FORMAT (A1)
      SCREEN = .FALSE.
      IF ((RESP .EQ. 'Y') .OR. (RESP .EQ. 'Y'))  SCREEN = .TRUE.
C
C  INITIALIZE POSITION DATA
C
      S = S0
C
      X = S0*SIN(INITGAM) + XOFFSET
      Y = S0*COS(INITGAM) + YOFFSET
C
      R  = SQRT( S*S + T*T - 2*S*T*COS(PI - INITGAM))
      AZ = ASIN (S/R * SIN(INITGAM))
C
      PITER  = NINT(TPRINT/TSAMPLE)
      PITER1 = PITER/5
      FTIME  = .TRUE.
      I = 1
C
C
C   TOP OF SIMULATION LOOP
C
  100 CONTINUE
C
         XOLD  = X
         YOLD  = Y
         AZOLD = AZ
C
C  CALCULATE NEW POSITION
C
         CALL WIND (VGND, UVGND, PSI)
C
         CALL POSITION (VGND, GAMMA, TSAMPLE, XOLD, YOLD, X, Y)
C
         S = SQRT( (X-XOFFSET)**2 + (Y-YOFFSET)**2)
C
         INTANG = ATAN((X-XOFFSET)/(Y-YOFFSET))
C
         R  = SQRT( S*S + T*T - 2*S*T*COS(PI - INTANG))
         AZ = ASIN( S/R * SIN(PI - INTANG))
C
C  CALCULATE ESTIMATED POSITION WHEN NEEDED FOR PRINTOUT
C
         IF ((MOD(I,PITER1) .EQ. 0) .OR.
     &        (S .LE. (4*TSAMPLE*VGND))) THEN
C
            AZDOT  = (AZOLD - AZ)/TSAMPLE
C
            VGEST  = VGND - UVGND
            GAMEST = GAMMA - UGAMMA
```

```
            AZEST  = AZ - UAZ
C
            REST   = (VGEST / AZDOT * SIN (GAMEST - AZEST))
C
            DELTAR = (R - REST)
C
            CALL ERRORANALYSIS (AZ, AZDOT, AZOLD, VGND)
C
            IF (AZ*RAD .GT. 0.1) THEN
               WRITE(18,175) AZ*RAD, R, REST, R+SIGMAR, R-SIGMAR
  175          FORMAT(F7.2, 4F10.1)
            END IF
C
C  PRINT OUT IF REQUESTED, OR IF NEAR COMPLETION
C
            IF ((MOD(I,PITER) .EQ. 0) .OR.
     &          (S .LE. (4*TSAMPLE*VGND))) THEN
C
               CALL PRNT(R, REST, DELTAR, S, AZ, INITGAM, FTIME,
     &                   SCREEN, I, VGND, PSI, SPATH)
C
               FTIME = .FALSE.
            END IF
         END IF
C
         I = I+1
C
      IF ((S .GT. (4*TSAMPLE*VGND)) .OR. (Y .LT. YOFFSET)) GO TO 100
C
      WRITE(18,175) 9999.99, T
C
      WRITE (*,45)
      WRITE (*,200)
  200 FORMAT(' Do you want to calculate for ',
     &       'different error values? <Y>')
      READ (*,45) RESP
      IF (RESP .NE. 'N') GO TO 1
C
      CLOSE (15)
      CLOSE (16)
      CLOSE (17)
      CLOSE (18)
C
      STOP
      END
```

A.2 Subroutines for Simulation Program

```
C  THIS SUBROUTINE READS IN ALL OF THE DATA FROM THE INPUT DATA FILE
C
      SUBROUTINE READIN (XOFFSET, YOFFSET, SPATH)
C
      REAL SO, GAMMA, T, VAIR, VWIND, DWIND, TSAMPLE, TPRINT,
     &     XOFFSET, YOFFSET,
     &     UVAIR, UVWIND, UDWIND, UAZ, UGAMMA, UTSAMPLE
C
      CHARACTER COMMENT*4
C
      COMMON /DATA/ SO, GAMMA, T, VAIR, VWIND, DWIND, TSAMPLE,
     &              TPRINT, UVAIR, UVWIND, UDWIND, UGAMMA,
     &              UAZ, UTSAMPLE
C
      REAL A, E, K, P, YO
C
      COMMON /COURSE/ A(6), E(6), K, P, YO
C
      INTEGER I
C
      LOGICAL SPATH
C
      RAD = 57.29578
C
C   READ IN THE COEFFICIENTS OF THE GROUND PATH
C
      READ (15,10) COMMENT
      READ (15,20) (A(I),I=1,6)
C
C   CHECK IF PATH EXISTS
C
      DO 5 I=1,6
         IF (A(I) .NE. 0.0) SPATH = .TRUE.
    5 CONTINUE
C
C   READ IN THE EXPONENTS FOR THE GROUND PATH
C
      READ (15,10) COMMENT
      READ (15,20) (E(I), I=1,6)
C
C   READ IN THE CONSTANT MULTIPLIER FOR THE GROUND PATH
C
      READ (15,10) COMMENT
      READ (15,20) K
C
C   READ IN THE TOTAL EXPONENT FOR THE GROUND PATH
C
      READ (15,10) COMMENT
      READ (15,20) P
C
C   READ IN THE Y OFFSET FOR THE GROUND PATH
C
```

```
      READ (15,10) COMMENT
      READ (15,20) YO
C
C   READ IN THE X AND Y OFFSETS OF THE RUNWAY
C
      READ (15,10) COMMENT
      READ (15,20) XOFFSET, YOFFSET
C
C   READ IN THE DISTANCE FROM MARKER TO AIRCRAFT
C
      READ(15,10) COMMENT
      READ(15,20) SO
C
C   READ IN THE ANGLE BETWEEN RUNWAY CENTER LINE AND AIRCRAFT COURSE
C
      READ(15,10) COMMENT
      READ(15,20) GAMMA
      GAMMA = GAMMA / RAD
C
C   READ IN THE DISTANCE FROM RUNWAY TO MARKER
C
      READ(15,10) COMMENT
      READ(15,20) T
C
C   READ IN THE AIRSPEED
C
      READ(15,10) COMMENT
      READ(15,20) VAIR
C
C   READ IN WIND VELOCITY
C
      READ(15,10) COMMENT
      READ(15,20) VWIND
C
C   READ IN WIND DIRECTION
C
      READ(15,10) COMMENT
      READ(15,20) DWIND
      DWIND = DWIND / RAD
C
C   READ IN SAMPLE TIME
C
      READ(15,10) COMMENT
      READ(15,20) TSAMPLE
C
C   READ IN TIME BETWEEN PRINTOUTS
C
      READ(15,10) COMMENT
      READ(15,20) TPRINT
      IF (TPRINT .LT. TSAMPLE) TPRINT = TSAMPLE
C
C   READ IN UNCERTAINTY IN AIRSPEED
```

```
C
      READ(15,10) COMMENT
      READ(15,20) UVAIR
C
C   READ IN UNCERTAINTY IN WIND SPEED
C
      READ(15,10) COMMENT
      READ(15,20) UVWIND
C
C   READ IN UNCERTAINTY IN WIND DIRECTION
C
      READ(15,10) COMMENT
      READ(15,20) UDWIND
      UDWIND = UDWIND / RAD
C
C   READ IN UNCERTAINTY IN GAMMA
C
      READ(15,10) COMMENT
      READ(15,20) UGAMMA
      UGAMMA = UGAMMA / RAD
C
C   READ IN UNCERTAINTY IN AZIMUTH ANGLE
C
      READ(15,10) COMMENT
      READ(15,20) UAZ
      UAZ = UAZ / RAD
C
C   READ IN UNCERTAINTY IN SAMPLE TIME
C
      READ(15,10) COMMENT
      READ(15,20) UTSAMPLE
C
   10 FORMAT(A4)
   20 FORMAT(6F13.6)
C
      RETURN
      END
C
C
C
C
C  THIS SUBROUTINE PRINTS OUT THE INPUT DATA AND ALLOWS ANY OF IT
C  TO BE CORRECTED IF IT IS NOT ALREADY CORRECT
C
      SUBROUTINE CORRECT(INITGAM)
C
      REAL C(14)
C
      INTEGER RESP
C
      REAL SO, GAMMA, T, VAIR, VWIND, DWIND, TSAMPLE, INITGAM,
     &     TPRINT, UVAIR, UVWIND, UDWIND, UGAMMA, UAZ, UTSAMPLE
```

```
C
      COMMON /DATA/ S0, GAMMA, T, VAIR, VWIND, DWIND, TSAMPLE,
     &              TPRINT, UVAIR, UVWIND, UDWIND, UGAMMA,
     &              UAZ, UTSAMPLE
C
      RAD = 57.29578
C
      C(1) = S0
      C(2) = INITGAM*RAD
      C(3) = T
      C(4) = VAIR
      C(5) = VWIND
      C(6) = DWIND*RAD
      C(7) = TSAMPLE
      C(8) = TPRINT
      C(9) = UVAIR
      C(10) = UVWIND
      C(11) = UDWIND*RAD
      C(12) = UGAMMA*RAD
      C(13) = UAZ*RAD
      C(14) = UTSAMPLE
C
      WRITE (*,10) C(1), C(8), C(2), C(9), C(3),
     &              C(10), C(4), C(11), C(5), C(12),
     &              C(6), C(13), C(7), C(14)
C
   10 FORMAT(//,'   1. Intercept   :',F10.0,4X,'8. Print Time  :',
     & F10.2,/,
     &     '   2. Gamma       :',F10.2,4X,'9.  Error V air :',F10.2,/,
     &     '   3. Marker Dist.:',F10.0,4X,'10. Error Wind  :',F10.2,/,
     &     '   4. Airspeed    :',F10.2,4X,'11. Error W dir :',F10.2,/,
     &     '   5. Wind speed  :',F10.2,4X,'12. Error Gamma :',F10.2,/,
     &     '   6. Wind direct.:',F10.2,4X,'13. Error Azmth :',F10.2,/,
     &     '   7. Sample Time :',F10.3,4X,'14. Error Time  :',F10.3,/,
     &         /)
C
  100  WRITE(*,20)
   20  FORMAT(' Type in the number to change. (<CR>=done)')
       READ(*,30, ERR=100) RESP
    30 FORMAT(I2)
       IF (RESP .NE. 0)  THEN
          WRITE(*,40)  C(RESP)
   40     FORMAT(' Current value is :',F12.3,'    New value is ?')
          READ(*,50) C(RESP)
   50     FORMAT(F12.0)
          GO TO 100
       END IF
C
       S0 = C(1)
       INITGAM = C(2)/RAD
       T = C(3)
       VAIR = C(4)
```

```
      VWIND = C(5)
      DWIND = C(6)/RAD
      TSAMPLE = C(7)
      TPRINT = C(8)
      UVAIR = C(9)
      UVWIND = C(10)
      UDWIND = C(11)/RAD
      UGAMMA = C(12)/RAD
      UAZ = C(13)/RAD
      UTSAMPLE = C(14)
      RETURN
      END
C
C
C
C
C  THIS SUBROUTINE PRINTS OUT THE DATA AT EACH POINT.
C  IT ALSO PRINTS OUT THE HEADER FOR THE DATA
C
      SUBROUTINE PRNT(R, REST, DELTAR, S, AZ, INITGAM,
     &                FTIME, SCREEN, I, VGND, PSI, SPATH)
C
      INTEGER I, J
C
      REAL R, REST, DELTAR, RTOVG, RTOGAM, RTOAZ, RTOAZDOT
C
      REAL UAZ,  UGAMMA,  RAD, S0, INITGAM,
     &     UVAIR, UVWIND, UDWIND, UTSAMPLE,
     &     TPRINT, VWIND, DWIND,
     &     S, T, VAIR, VGND, GAMMA, PSI, TSAMPLE
C
      LOGICAL FTIME, SCREEN, SPATH
C
      COMMON /DATA/ S0, GAMMA, T, VAIR, VWIND, DWIND, TSAMPLE,
     &              TPRINT, UVAIR, UVWIND, UDWIND, UGAMMA,
     &              UAZ, UTSAMPLE
C
      COMMON /ANALYSIS/ RTOVG, RTOGAM, RTOAZ, RTOAZDOT, SIGMAR
C
      COMMON /COURSE/ A(6), E(6), K, P, Y0
C
      REAL A, E, K, P, Y0
C
      RAD = 57.29578
      IF (FTIME) THEN
         IF (SCREEN) THEN
            WRITE(*,5)'R (ft)','R est (ft)','Delta R (ft)',
     &                'Intcpt. (ft)','Azimuth(deg)',
     &                'R to G (sec)','R to Gam(ft)','R to Az (ft)',
     &                'R to Azdot'
    5       FORMAT(5A13)
         END IF
```

```
C
C
      WRITE(16,1000) VAIR, PSI*RAD, VGND, INITGAM*RAD,
     &               VWIND, DWIND*RAD,
     &               S0, T, TSAMPLE
      IF (SPATH) THEN
         WRITE(16,1005) (A(J),J=1,6),(E(J),J=1,6),K,P,Y0
      ELSE
         WRITE(16,1006)
      END IF
      WRITE(16,1010) UVAIR, UGAMMA*RAD, UVWIND, UDWIND*RAD,
     &               UAZ*RAD, UTSAMPLE
C
C
      WRITE(17,1000) VAIR, PSI*RAD, VGND, INITGAM*RAD,
     &               VWIND, DWIND*RAD,
     &               S0, T, TSAMPLE
      IF (SPATH) THEN
         WRITE(17,1005) (A(J),J=1,6),(E(J),J=1,6),K,P,Y0
      ELSE
         WRITE(17,1006)
      END IF
      WRITE(17,1010) UVAIR, UGAMMA*RAD, UVWIND, UDWIND*RAD,
     &               UAZ*RAD, UTSAMPLE
C
C
      WRITE(16,10)  ' Time ','R      ','R est    ','Delta R   ',
     &              'Intercept ','Azimuth   '
      WRITE(16,10)  ' (sec)','(ft)    ','(ft)    ','(ft)    ',
     &              '(ft)    ','(deg)   '
C
C
      WRITE(17,10)  ' Time ','dR / dVg ','dR / dGamma',
     &              'dR / dAz ','dR / dAzdot ','Sigma R   '
      WRITE(17,10)  ' (sec)','(ft/ft/sec)','(ft/deg)  ','(ft/deg) ',
     &              '(ft/deg/s) ','(ft)    '
C
C
      END IF
C
   10 FORMAT(A6,6A13)
 1000 FORMAT(//,  ' Microwave Landing System Simulation ',//,
     &            ' Ind. Airspeed    : ',F10.2,' ft/sec ',
     &            ' Initial Heading  : ',F10.2,' deg    ',/,
     &            ' Ground Speed     : ',F10.2,' ft/sec ',
     &            ' Intcpt. Angle    : ',F10.2,' deg    ',/,
     &            ' Wind Speed       : ',F10.2,' ft/sec ',
     &            ' Wind Direction   : ',F10.2,' deg    ',/,
     &            ' Dist. to O.M.    : ',F10.0,' ft     ',
     &            ' O.M. to Runway   : ',F10.0,' ft     ',/,
     &            ' Sample Time      : ',F10.3,' sec    ',
     &      //)
```

```
 1005 FORMAT(' The ground path equation : Y = K(A*X**E+...)**P + Y0 ',
     &       ' is defined by :',//,
     &       ' A(1) = ',F10.2,'  A(2) = ',F10.2,'  A(3) = ',F10.2,/,
     &       ' A(4) = ',F10.2,'  A(4) = ',F10.2,'  A(6) = ',F10.2,/,
     &       ' E(1) = ',F10.4,'  E(2) = ',F10.4,'  E(3) = ',F10.4,/,
     &       ' E(4) = ',F10.4,'  E(4) = ',F10.4,'  E(6) = ',F10.4,/,
     &       ' K    = ',F10.4,'  P    = ',F10.4,'  Y0   = ',F10.2,//)
 1006 FORMAT(' A user defined ground course was used.',//)
 1010 FORMAT(' Airspeed Error    :',F10.2,' ft/sec ',
     &       ' Heading Error     :',F10.2,' deg    ',/,
     &       ' Wind speed Error  :',F10.2,' ft/sec ',
     &       ' Wind Dir. Error   :',F10.2,' deg    ',/,
     &       ' Azimuth Error     :',F10.2,' deg    ',
     &       ' Sample Time Error :',F10.3,' sec    ',/)
C
C
C
C     THIS IS PRINTED EVERY TIME
C
      IF (SCREEN) THEN
         WRITE (*,15) R, REST, DELTAR, S, AZ*RAD,
     &                RTOVG, RTOGAM, RTOAZ, RTOAZDOT
      END IF
      WRITE (16,20)   I*TSAMPLE,  R, REST, DELTAR, S, AZ*RAD
      WRITE (17,25)   I*TSAMPLE,  RTOVG, RTOGAM/RAD,
     &                RTOAZ/RAD, RTOAZDOT/RAD,
     &                SIGMAR
   15 FORMAT(/, 4F13.0, F13.2, /, F13.2, 3F13.0)
   20 FORMAT(F6.2, 4F13.0, F13.2)
   25 FORMAT(F6.2, F13.2, 4F13.0)
C
      RETURN
      END
C
C
C
C
C  THIS SUBROUTINE CALCULATES THE GROUND VELOCITY, THE UNCERTAINTY IN THE
C  GROUND VELOCITY, AND THE GROUND TRACK ANGLE BASED ON THE CURRENT VELOCITY
C  AND THE WIND VELOCITY
C
      SUBROUTINE WIND ( VGND, UVGND, PSI)
C
      REAL  GAMMA, VAIR, VWIND, DWIND, VGND, PSI, UVGND
C
      REAL S0,  T, TSAMPLE, TPRINT, UVAIR, UVWIND, UDWIND,
     &     UGAMMA, UAZ, UTSAMPLE
C
      COMMON /DATA/ S0, GAMMA, T, VAIR, VWIND, DWIND, TSAMPLE,
     &              TPRINT, UVAIR, UVWIND, UDWIND, UGAMMA,
     &              UAZ, UTSAMPLE
C
```

```
      VGND = VWIND * COS(DWIND - GAMMA)
     &      + SQRT( VAIR*VAIR - VWIND*VWIND*SIN(DWIND-GAMMA)*
     &                                  SIN(DWIND-GAMMA))
C
      PSI = ASIN((VGND*SIN(GAMMA) - VWIND*SIN(DWIND)) / VAIR)
C
      V1 = (VWIND+UVWIND)*COS((DWIND+UDWIND)-(GAMMA+UGAMMA))
     &    + SQRT( (VAIR+UVAIR)**2 - ((VWIND+UVWIND)**2 *
     &             (SIN((DWIND+UDWIND)-(GAMMA+UGAMMA)))**2))
C
      UVGND = VGND - V1
C
      RETURN
      END
C
C
C
C
C  THIS SUBROUTINE CALCULATES THE DERIVATIVES OF THE RANGE
C  WITH RESPECT TO THE GROUND VELOCITY, GAMMA, AZ, AND AZDOT
C  FOR STATISTICAL ERROR ANALYSIS
C
      SUBROUTINE ERRORANALYSIS (AZ, AZDOT, AZOLD, VGND)
C
      REAL AZ, AZDOT, AZOLD, VGND
C
      COMMON /ANALYSIS/ RTOVG, RTOGAM, RTOAZ, RTOAZDOT, SIGMAR
C
      COMMON /DATA/ S0, GAMMA, T, VAIR, VWIND, DWIND, TSAMPLE,
     &              TPRINT, UVAIR, UVWIND, UDWIND, UGAMMA,
     &              UAZ, UTSAMPLE
C
      REAL RTOVG, RTOGAM, RTOAZ, RTOAZDOT, SIGMAR,
     &     RTOTS, RTOAZOLD, RTOVAIR, RTOVWIND, RTODWIND,
     &     UVAIR, UVWIND, UDWIND, UAZ, UGAMMA, UTSAMPLE
C
      REAL VGTOVAIR, VGTOVWIND, VGTOGAMMA, VGTODWIND,
     &     S0, GAMMA, T, VAIR, VWIND, DWIND, TSAMPLW, TPRINT,
     &     DENOM
C
C
C     THIS DENOMINATOR IS USED OFTEN IN THE DERIVATIVES
C
      DENOM = SQRT(VAIR*VAIR - VWIND*VWIND*SIN(DWIND-GAMMA)*
     &                                  SIN(DWIND-GAMMA))
C
      RTOVG = SIN(GAMMA - AZ) / AZDOT
C
      RTOAZDOT = (-VGND * SIN(GAMMA - AZ)) / (AZDOT * AZDOT)
C
      VGTOVAIR = VAIR / DENOM
C
```

```
      VGTOVWIND = COS(DWIND-GAMMA) - VWIND*SIN(DWIND-GAMMA)*
     &                               SIN(DWIND-GAMMA) / DENOM
C
      VGTOGAM = VWIND*SIN(DWIND-GAMMA) - VWIND*VWIND*SIN(DWIND-GAMMA)
     &                                  *COS(DWIND-GAMMA) / DENOM
C
      VGTODWIND = -VGTOGAM
C
      RTOAZ = -VGND*COS(GAMMA-AZ) / AZDOT
     &                          -VGND*SIN(GAMMA-AZ) / AZDOT / TSAMPLE
C
      RTOGAM = RTOVG*VGTOGAM*SIN(GAMMA-AZ)/AZDOT +
     &         VGND*COS(GAMMA - AZ)/AZDOT
      RTOTS = (DENOM + VWIND*COS(DWIND-GAMMA))*SIN(GAMMA-AZ)/(AZOLD-AZ)
C
      RTOVAIR = RTOVG * VGTOVAIR
C
      RTOVWIND = RTOVG * VGTOVWIND
C
      RTODWIND = RTOVG * VGTODWIND
C
      SIGMAR = RTOVAIR * RTOVAIR * UVAIR * UVAIR
     &       + RTOVWIND * RTOVWIND * UVWIND * UVWIND
     &       + RTODWIND * RTODWIND * UDWIND * UDWIND
     &       + RTOAZ * RTOAZ * UAZ * UAZ
     &       + RTOGAM * RTOGAM * UGAMMA * UGAMMA
     &       + RTOTS * RTOTS * UTSAMPLE *UTSAMPLE
C
      SIGMAR = SQRT(SIGMAR)
C
      RETURN
      END
C
C
C
C  THIS SUBROUTINE CALCULATES THE NEW POSITION (X,Y) USING A SIMPLE
C  INTEGRATION TECHNIQUE.  THE FUNCTIONS PATH AND DPATH GIVE THE POSITION
C  AND THE DERIVATIVE ALONG THE GROUND PATH FOLLOWED.
C
      SUBROUTINE POSITION( VGND, GAMMA, DELTAT, XOLD, YOLD, X, Y)
C
      REAL VGND, DELTAT, XOLD, YOLD, X, Y, GAMMA,
     &     VX, VY, PI, SIGN
C
      PI = 3.14159265
C
      SIGN = -1.0
      IF ((GAMMA .GE. PI) .OR. (GAMMA .LT. 0.0))  SIGN = 1.0
C
      VX = SQRT(VGND*VGND/(DPATH(XOLD)*DPATH(XOLD)+1))
      VX = SIGN * VX
       X = VX*DELTAT + XOLD
```

```
       Y = PATH(X)
      VY = SQRT(VGND*VGND - VX*VX)
C
      GAMMA = PI/2.0 - ATAN(DPATH(X))
C
      RETURN
      END
```

A.3 Path and DPath Functions for General Polynomial Ground Path Including Straight Lines

```
      REAL FUNCTION PATH(X)
C
C    THIS FUNCTION IS THE EQUATION OF THE GROUND PATH BASED ON
C    THE EQUATION
C
C    Y = A(1)*X**E(1) + A(2)*X**E(2) + ...
C
      REAL X, K, P, A, E, Y0
C
      INTEGER I
C
      COMMON /COURSE/ A(6), E(6), K, P, Y0
C
      PATH = 0
C
      DO 10 I=1,6
         IF ((E(I) .LT. 0.000001).AND.(E(I) .GT. -0.000001)) THEN
            PATH = PATH + A(I)
         ELSE
            PATH = PATH + A(I)*(X**E(I))
         END IF
   10 CONTINUE
C
      IF ((P .LT. 0.000001) .AND. (P .GT. -0.000001)) THEN
         PATH = K
      ELSE
         PATH = K * (PATH ** P)
      END IF
C
      PATH = PATH + Y0
C
      RETURN
      END
C
C
C
C
      REAL FUNCTION DPATH(X)
C
C    THIS IS THE DERIVATIVE OF THE FUNCTION DECLARED IN PATH
C
      REAL X, K, P, A, E, DTEMP, Y0
C
      INTEGER I
C
      COMMON /COURSE/ A(6), E(6), K, P, Y0
C
C
      DPATH = 0
C
      DO 10 I=1,6
         IF ((E(I) .LT. 0.000001).AND.(E(I) .GT. -0.000001)) THEN
```

```
            DPATH = DPATH + A(I)
         ELSE
            DPATH = DPATH + A(I)*(X**E(I))
         END IF
   10 CONTINUE
C
      IF ((P .LT. 1.000001) .AND. (P .GT. 0.999999)) THEN
         DPATH = 1
      ELSE
         DPATH = DPATH**(P-1.0)
      END IF
C
      DTEMP = 0
C
      DO 20 I=1,6
         IF ((E(I) .LT. 1.000001) .AND. (E(I) .GT. 0.999999)) THEN
            DTEMP = DTEMP + A(I)*E(I)
         ELSE
            DTEMP = DTEMP + A(I)*E(I)*(X**(E(I)-1.0))
         END IF
   20 CONTINUE
C
      DPATH = K * P * DPATH * DTEMP
C
C    THIS IS THE EQUATION THAT THIS FUNCTION IS SOLVING
C       DPATH = K * P * ( A(1)*X**E(1) + A(2)*X**E(2)
C     &                 + A(3)*X**E(3) + A(4)*X**E(4)
C     &                 + A(5)*X**E(5) + A(6)*X**E(6) )**(P-1.0)
C     &               * ( A(1)*E(1)*X*(E(1)-1.0)
C     &                 + A(2)*E(2)*X*(E(2)-1.0)
C     &                 + A(3)*E(3)*X*(E(3)-1.0)
C     &                 + A(4)*E(4)*X*(E(4)-1.0)
C     &                 + A(5)*E(5)*X*(E(5)-1.0)
C     &                 + A(6)*E(6)*X*(E(6)-1.0))
C
      RETURN
      END
```

A.4 Path and DPath Functions for Path #1 (Large Circular Arc)

```
      REAL FUNCTION PATH(X)
C
C     THIS FUNCTION IS THE EQUATION OF THE GROUND PATH FOR
C     PATH #1, A LARGE CIRCLE
C
      REAL X
C
      PATH = SQRT((14796.0)**2 - (X-14796.0)**2)
C
      RETURN
      END
C
C
C
C
      REAL FUNCTION DPATH(X)
C
C     THIS IS THE DERIVATIVE OF THE FUNCTION DECLARED IN PATH
C
      REAL X
C
      DPATH = (14796.0-X)/PATH(X)
C
      RETURN
      END
```

A.5 Path and DPath Functions for Path #2 (90° Straight Segment Followed by Circular Arc)

```
      REAL FUNCTION PATH(X)
C
C    THIS FUNCTION IS THE EQUATION OF GROUND PATH #1
C    IT IS A STRAIGHT SEGMENT FOLLOWED BY A CIRCULAR ARC
C
      REAL X
C
      IF (X .GE. 6576.) THEN
         PATH = 6576.0
      ELSE
         PATH = SQRT((6576.0)**2 - (X-6576.0)**2)
      END IF
C
      RETURN
      END
C
C
C
C
      REAL FUNCTION DPATH(X)
C
C    THIS IS THE DERIVATIVE OF THE FUNCTION DECLARED IN PATH
C
      REAL X
C
      IF (X .GE. 6576.) THEN
         DPATH = 0.0
      ELSE
         DPATH = (6576.0-X)/PATH(X)
      END IF
C
      RETURN
      END
```

A.6 Example Input File

```
****  COEFFICIENTS OF THE GROUND PATH EQUATION
1.73205
****  EXPONENTS OF THE GROUND PATH EQUATION
1.0
****  CONSTANT MULTIPLIER FOR GROUND PATH EQUATION
1.0
****  TOTAL EXPONENT FOR THE GROUND PATH EQUATION
1.0
****   YO  THE Y OFFSET FOR THE GROUND PATH EQUATION
0.0
****  XOFFSET AND YOFFSET OF THE END OF THE RUNWAY
0.0           0.0
****    SO     DISTANCE FROM AIRCRAFT TO MARKER
25000.
****   GAMMA    ANGLE BETWEEN RUNWAY CENTER LINE AND AIRCRAFT COURSE
30.0
****   T   DISTANCE FROM RUNWAY TO MARKER
12500.
****   VA  AIRSPEED
160.
****  VWIND  WIND SPEED
0.0
****  DWIND  WIND DIRECTION
0.0
****  TSAMPLE    SAMPLE TIME
0.1
****  TPRINT    TIME BETWEEN PRINT OUTS
5.0
****  UVAIR   UNCERTAINTY IN AIR SPEED
0.0
****  UVWIND  UNCERTAINTY IN WIND SPEED
0.0
****  UDWIND  UNCERTAINTY IN WIND DIRECTION
0.0
****  UGAMMA  UNCERTAINTY IN GROUND COURSE
0.0
****  UAZ  UNCERTAINTY IN AZIMUTH ANGLE
0.0
****  UTSAMPLE  UNCERTAINTY IN SAMPLE TIME
0.0
```

A.7 Example Output File

Microwave Landing System Simulation

Ind. Airspeed	:	160.00 ft/sec	Initial Heading	:	30.00 deg
Ground Speed	:	160.00 ft/sec	Intcpt. Angle	:	30.00 deg
Wind Speed	:	0.00 ft/sec	Wind Direction	:	0.00 deg
Dist. to O.M.	:	25000. ft	O.M. to Runway	:	25000. ft
Sample Time	:	0.200 sec			

The ground path equation : Y = K(A*X**E+...)**P + Y0 is defined by :

A(1) =	1.73	A(2) =	0.00	A(3) =	0.00
A(4) =	0.00	A(4) =	0.00	A(6) =	0.00
E(1) =	1.0000	E(2) =	0.0000	E(3) =	0.0000
E(4) =	0.0000	E(4) =	0.0000	E(6) =	0.0000
K =	1.0000	P =	1.0000	Y0 =	0.00

Airspeed Error	:	5.00 ft/sec	Heading Error	:	0.00 deg
Wind speed Error	:	0.00 ft/sec	Wind Dir. Error	:	0.00 deg
Azimuth Error	:	0.00 deg	Sample Time Error	:	0.000 sec

Time (sec)	R (ft)	R est (ft)	Delta R (ft)	Intercept (ft)	Azimuth (deg)
5.00	47524.	49041.	-1517.	24200.	14.75
10.00	46753.	48245.	-1493.	23400.	14.49
15.00	45982.	47451.	-1469.	22600.	14.23
20.00	45213.	46657.	-1444.	21800.	13.95
25.00	44445.	45865.	-1420.	21000.	13.67
30.00	43678.	45074.	-1396.	20200.	13.37
35.00	42912.	44284.	-1372.	19400.	13.06
40.00	42147.	43495.	-1348.	18600.	12.75
45.00	41384.	42708.	-1324.	17800.	12.42
50.00	40622.	41922.	-1301.	17000.	12.08
55.00	39861.	41138.	-1277.	16200.	11.72
60.00	39102.	40355.	-1253.	15400.	11.36
65.00	38345.	39575.	-1229.	14600.	10.97
70.00	37590.	38795.	-1206.	13800.	10.58
75.00	36836.	38018.	-1182.	13000.	10.16
80.00	36085.	37243.	-1158.	12200.	9.73
85.00	35335.	36470.	-1135.	11400.	9.28
90.00	34588.	35700.	-1112.	10600.	8.81
95.00	33844.	34932.	-1088.	9800.	8.32
100.00	33102.	34166.	-1065.	9000.	7.81
105.00	32362.	33404.	-1042.	8200.	7.28
110.00	31626.	32644.	-1019.	7400.	6.72
115.00	30893.	31888.	-996.	6600.	6.13
120.00	30163.	31135.	-973.	5800.	5.52
125.00	29436.	30386.	-950.	5000.	4.87
130.00	28714.	29641.	-927.	4200.	4.19
135.00	27996.	28901.	-904.	3400.	3.48

140.00	27283.	28165.	-882.	2600.	2.73
145.00	26574.	27434.	-860.	1800.	1.94
150.00	25871.	26708.	-837.	1000.	1.11
155.00	25173.	25989.	-815.	200.	0.23
155.60	25090.	25903.	-813.	104.	0.12

APPENDIX B

This appendix contains the plots of estimated range error versus range for all the cases studied. These are organized as follows:

Figure B.1 (a-f)	GA 160 ft/sec 30° intercept at 12,500 ft
Figure B.2 (a-f)	GA 160 ft/sec 45° intercept at 12,500 ft
Figure B.3 (a-f)	GA 160 ft/sec 30° intercept at 25,000 ft
Figure B.4 (a-f)	GA 160 ft/sec 45° intercept at 25,000 ft
Figure B.5	Commercial airline 236 ft/sec 30° intercept at 12,500 ft
Figure B.6	Commercial airline 236 ft/sec 45° intercept at 12,500 ft
Figure B.7	Commercial airline 236 ft/sec 30° intercept at 25,000 ft
Figure B.8	Commercial airline 236 ft/sec 45° intercept at 25,000 ft
Figure B.9	Commercial airline 236 ft/sec Trajectory 1
Figure B.10	Commercial airline 236 ft/sec Trajectory 2

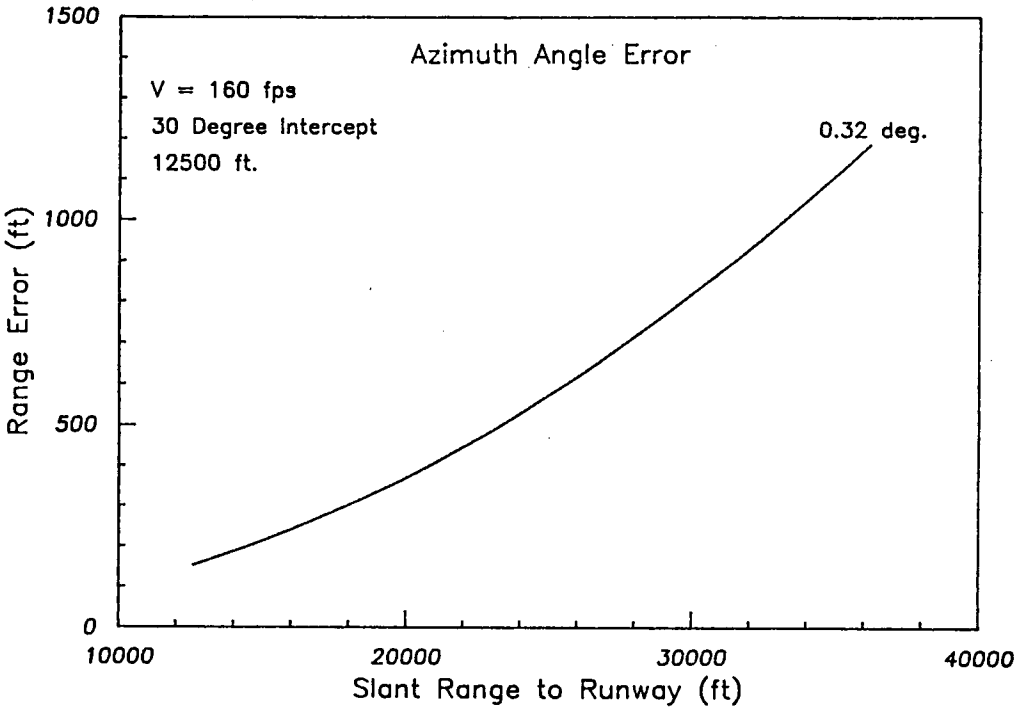

Figure B.1a: Range Estimation Error Due to Azimuth Angle Error for Constant Intercept Trajectory

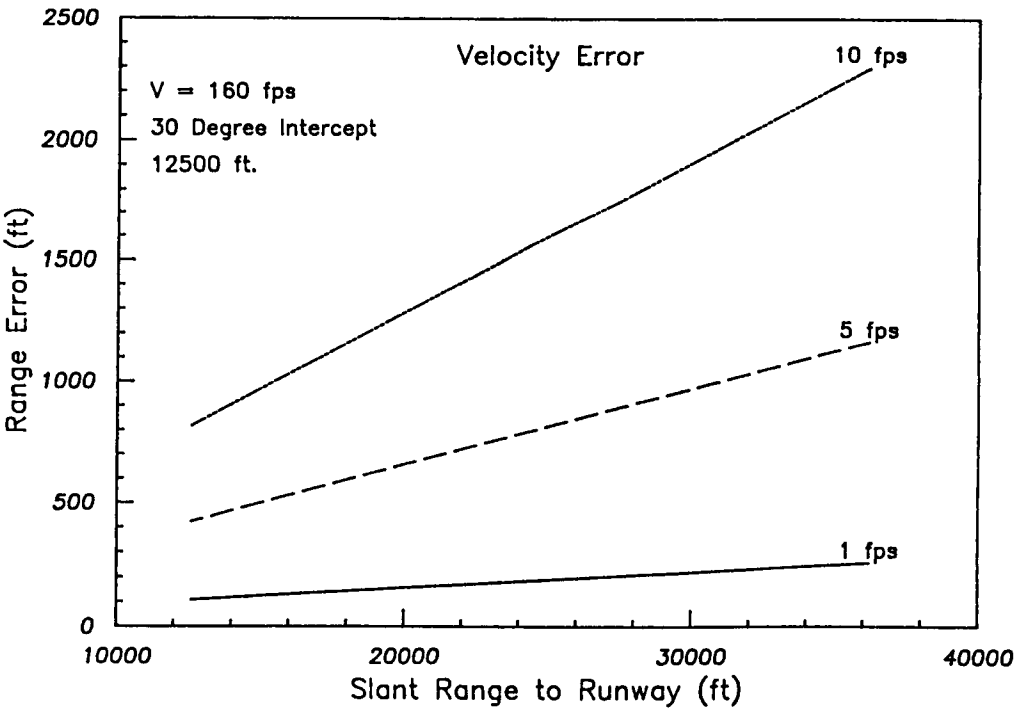

Figure B.1b: Range Estimation Error Due to Airspeed Sensor Errors

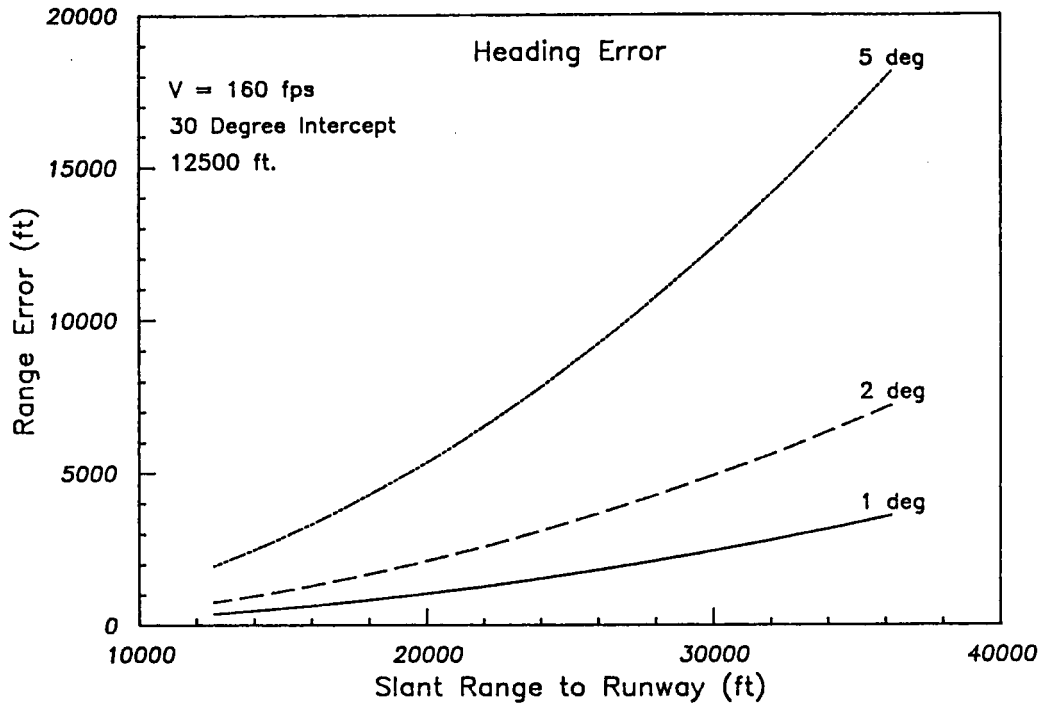

Figure B.1c: Range Estimation Error Due to Heading Sensor Error

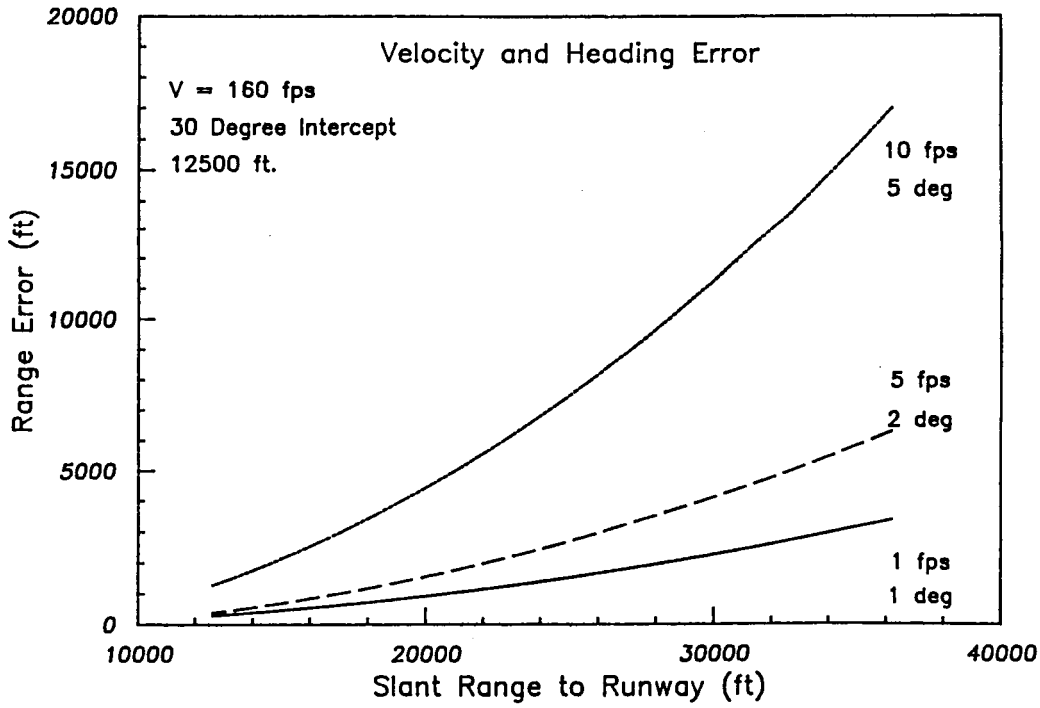

Figure B.1d: Range Estimation Error Due to Airspeed and Heading Sensor Errors

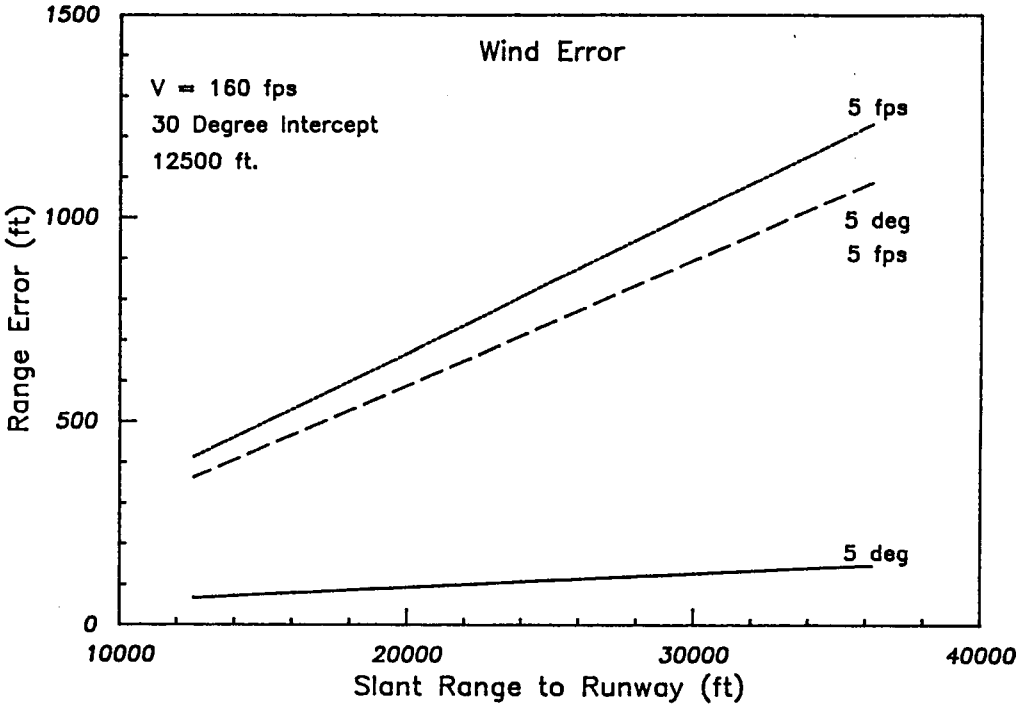

Figure B.1e: Range Estimation Error Due to Uncertainties in Wind Information. Nominal Wind: 20 fps from 135 deg.

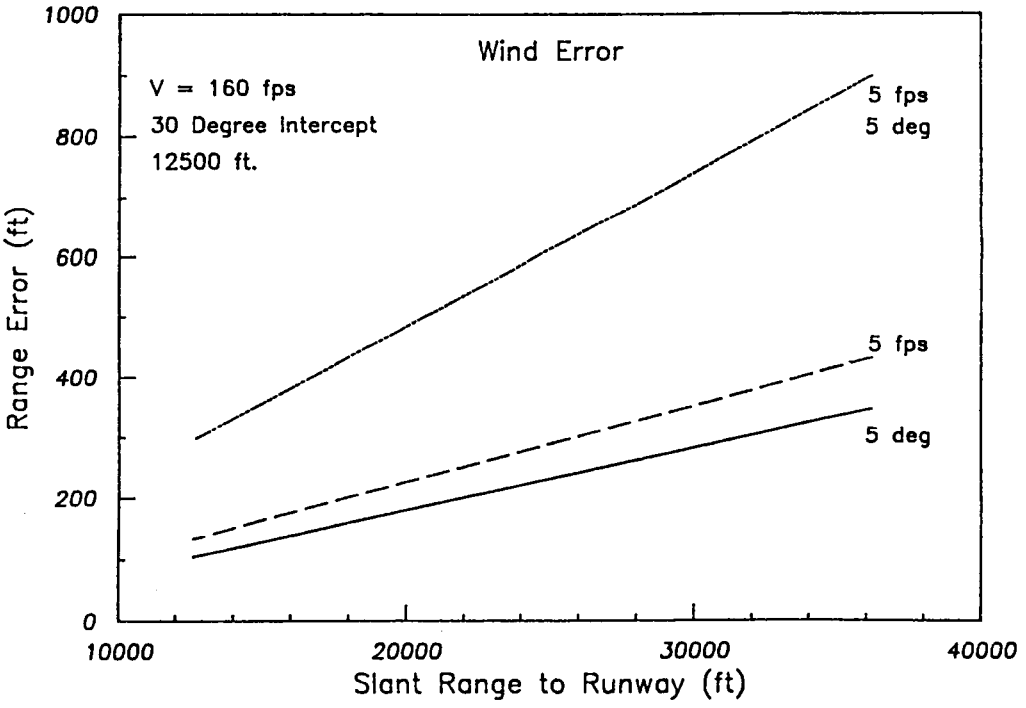

Figure B.1f: Range Estimation Error Due to Uncertainties in Wind Information. Nominal Wind: 20 fps from 225 deg.

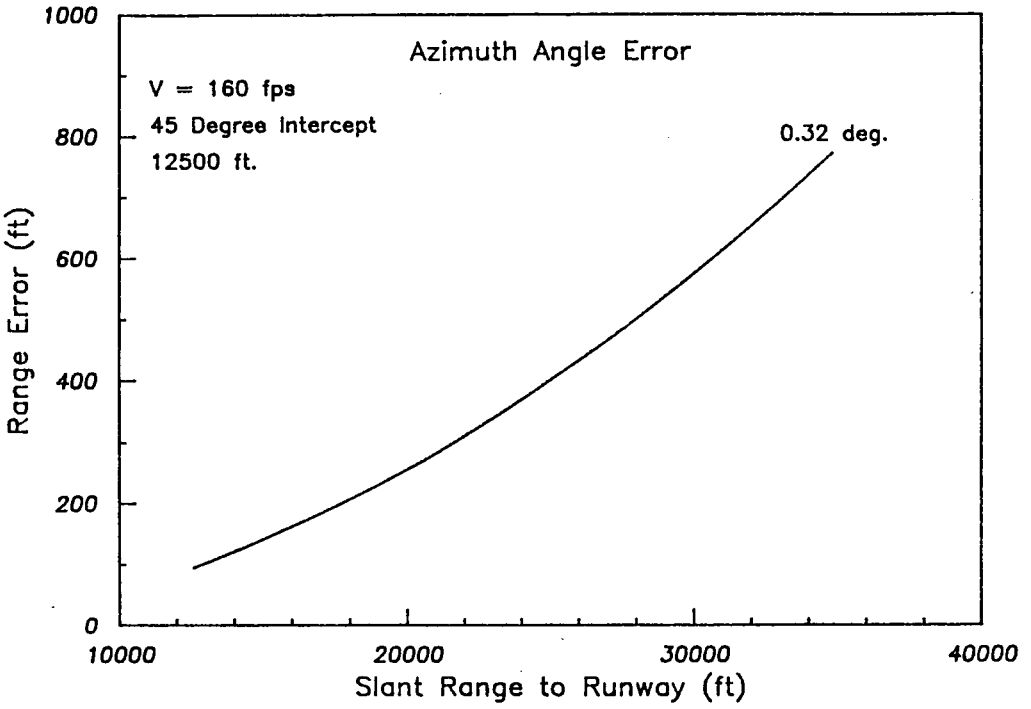

Figure B.2a: Range Estimation Error Due to Azimuth Angle Error for Constant Intercept Trajectory

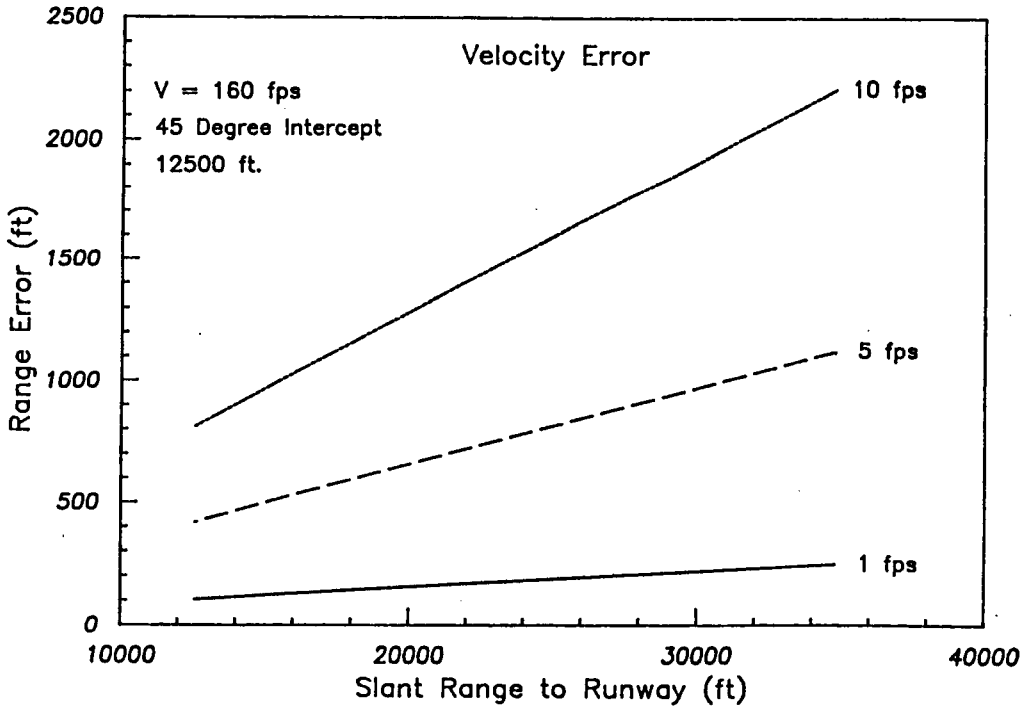

Figure B.2b: Range Estimation Error Due to Airspeed Sensor Errors

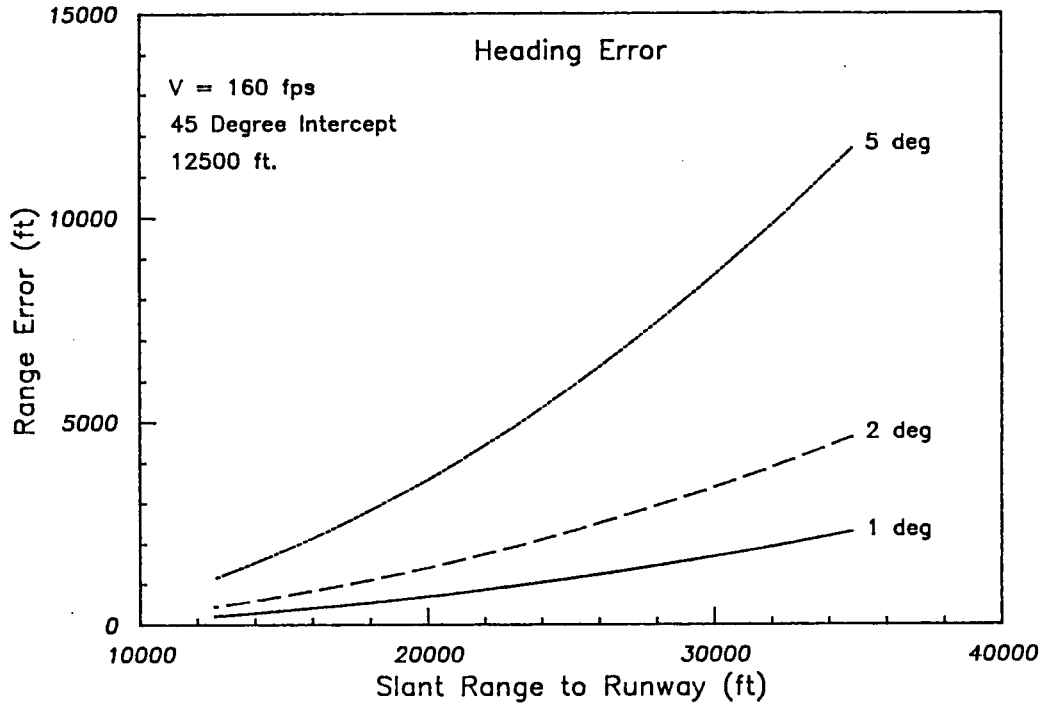

Figure B.2c: Range Estimation Error Due to Heading Sensor Error

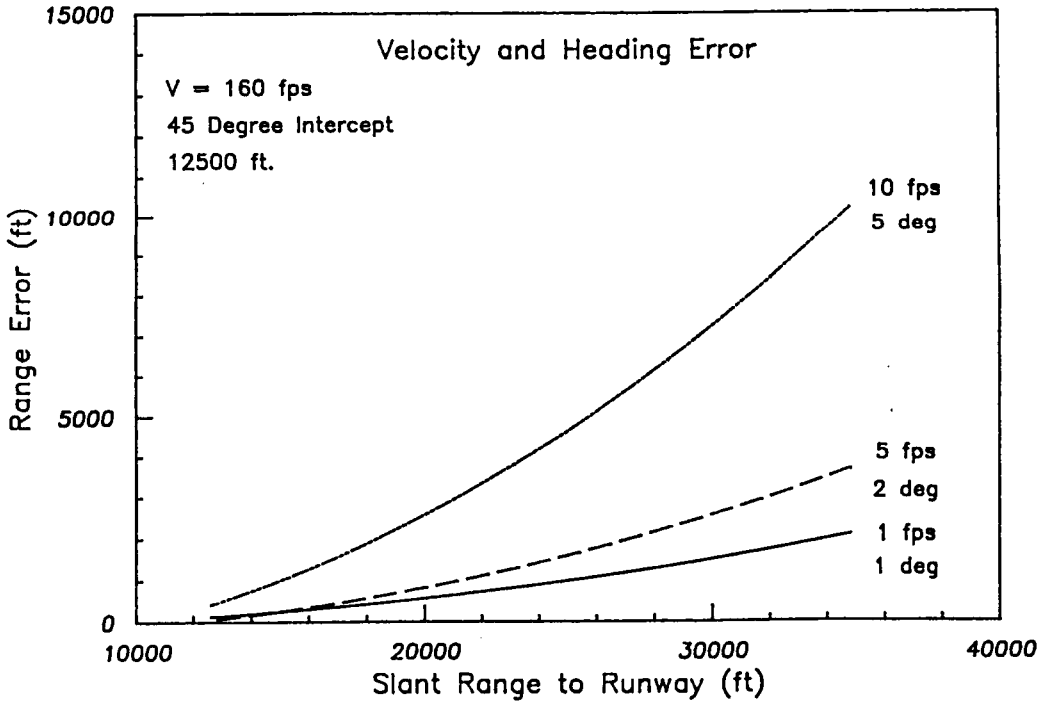

Figure B.2d: Range Estimation Error Due to Airspeed and Heading Sensor Errors

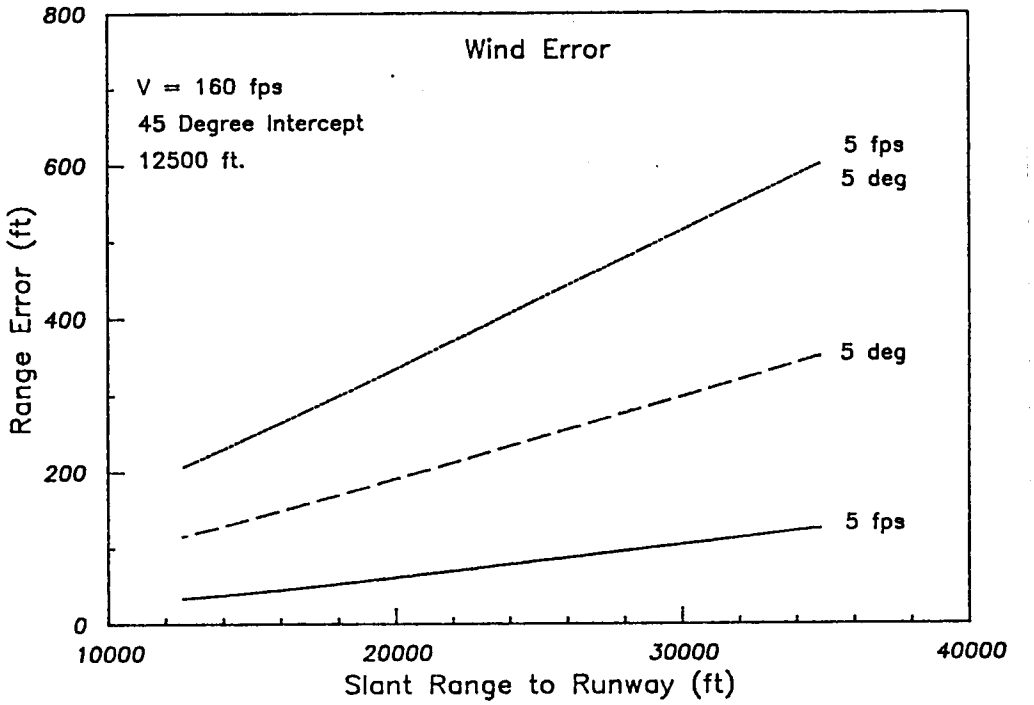

Figure B.2e: Range Estimation Error Due to Uncertainties in Wind Information. Nominal Wind: 20 fps from 135 deg.

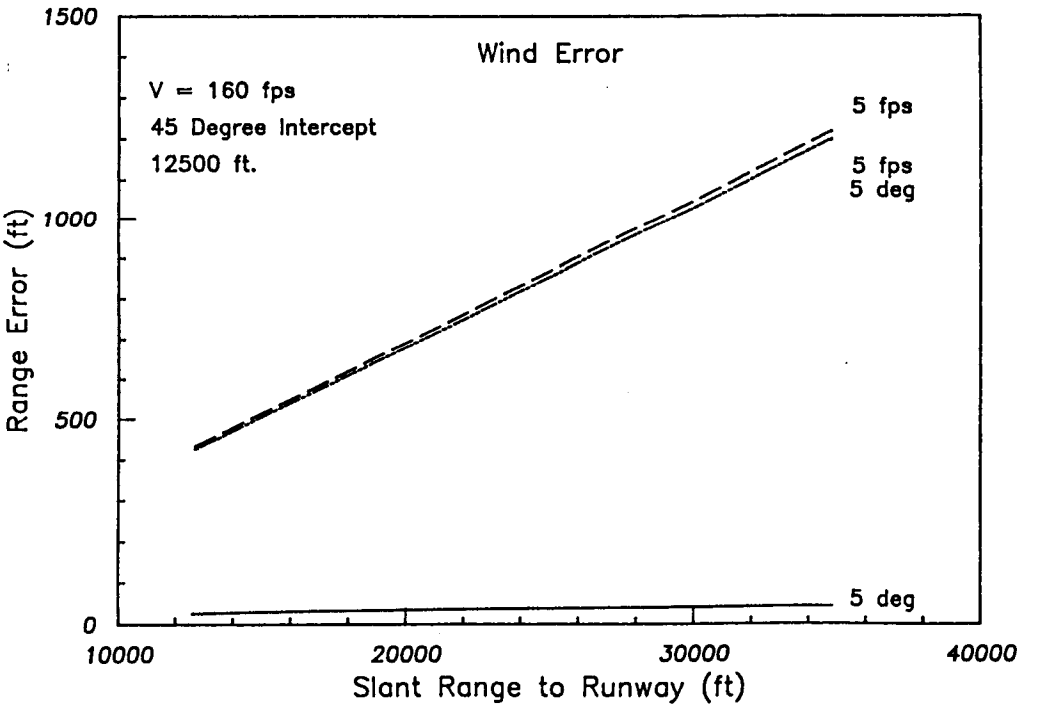

Figure B.2f: Range Estimation Error Due to Uncertainties in Wind Information. Nominal Wind: 20 fps from 225 deg.

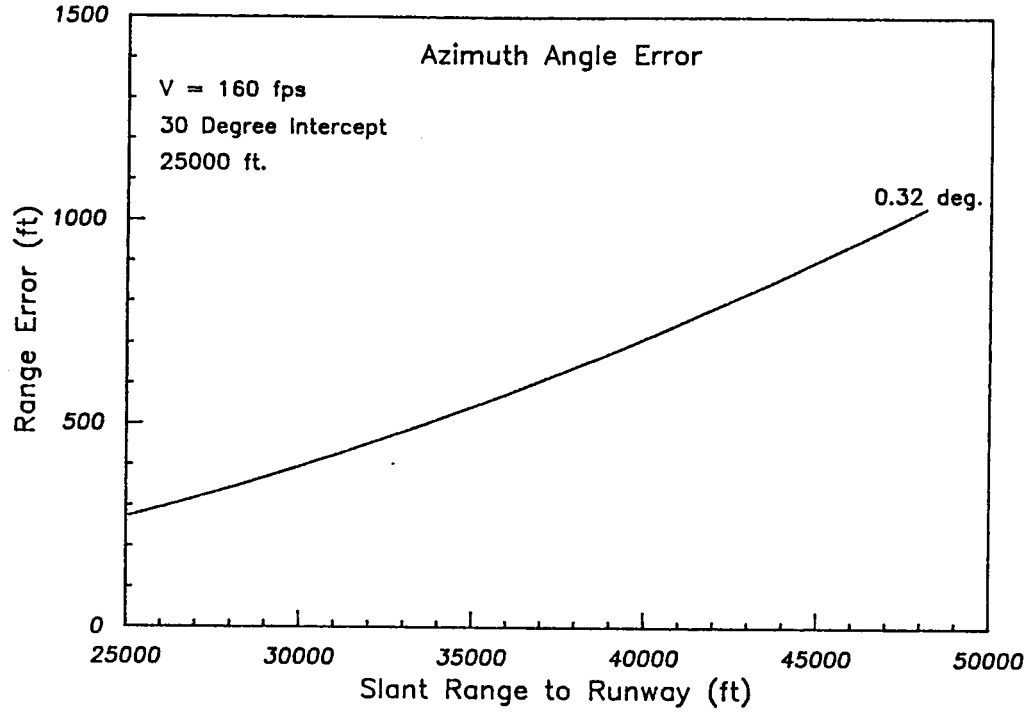

Figure B.3a: Range Estimation Error Due to Azimuth Angle Error for Constant Intercept Trajectory

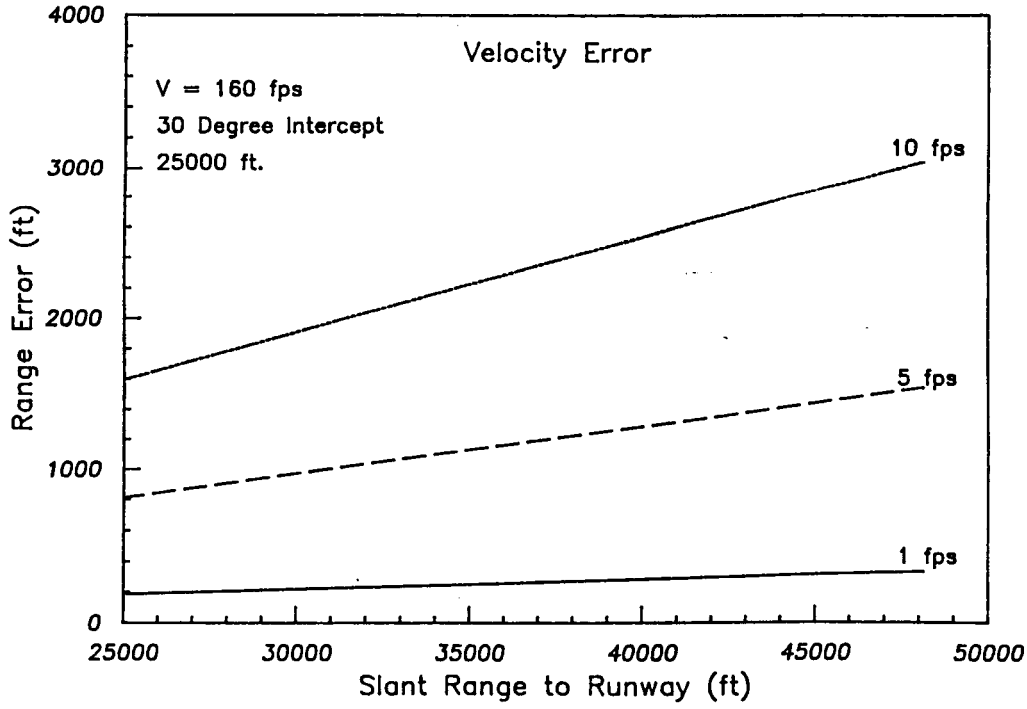

Figure B.3b: Range Estimation Error Due to Airspeed Sensor Errors

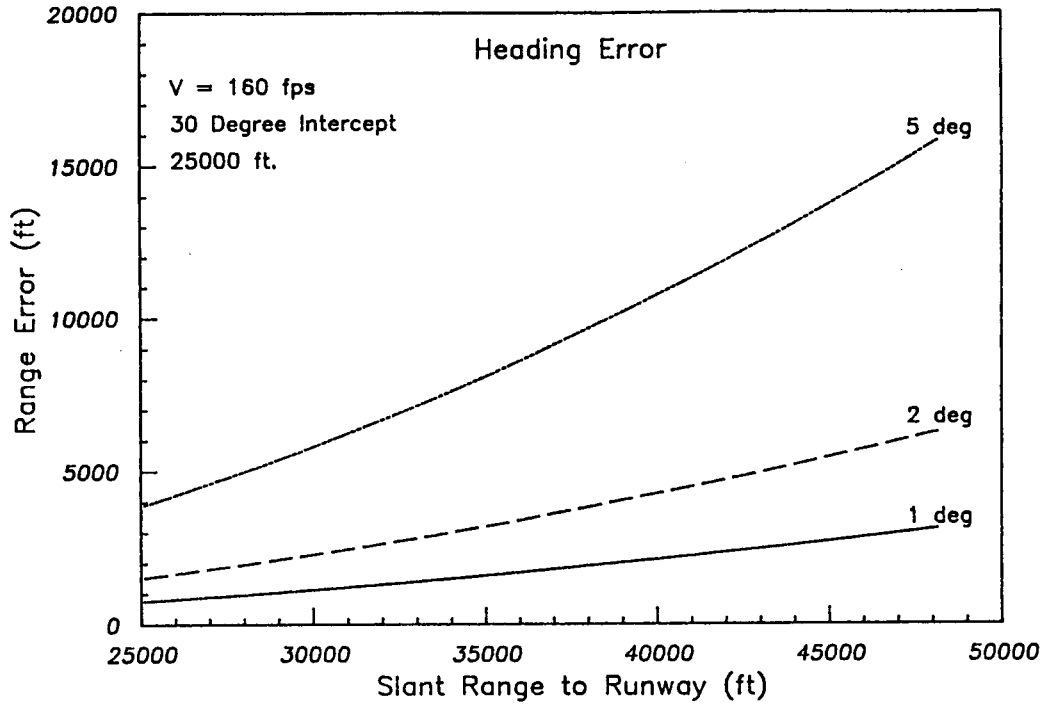

Figure B.3c: Range Estimation Error Due to Heading Sensor Error

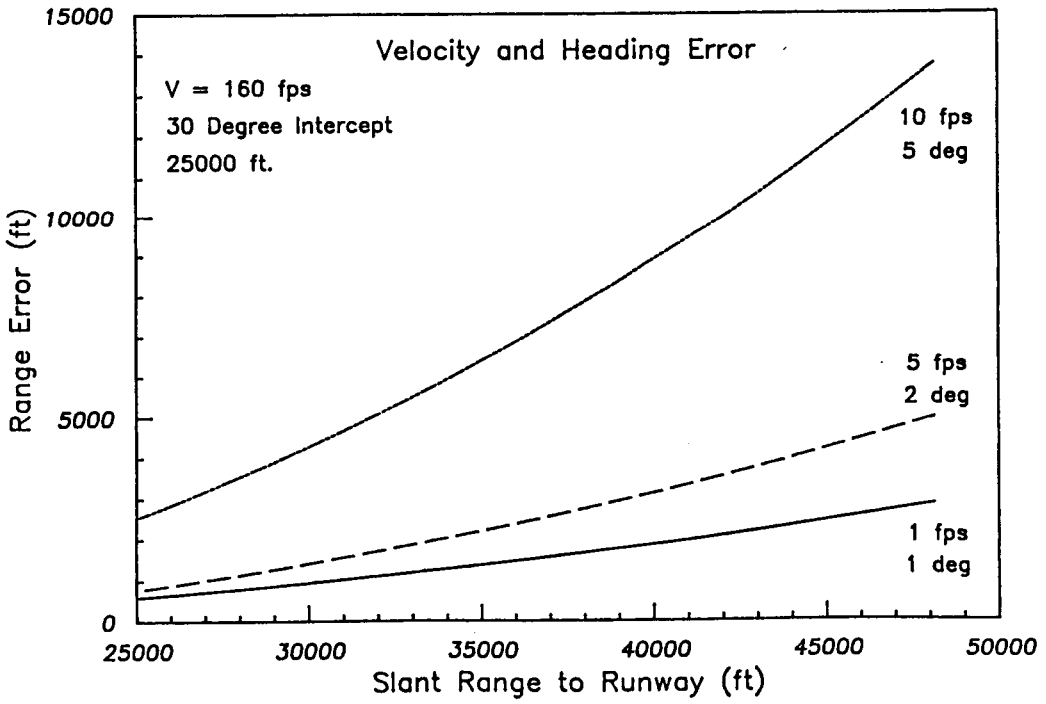

Figure B.3d: Range Estimation Error Due to Airspeed and Heading Sensor Errors

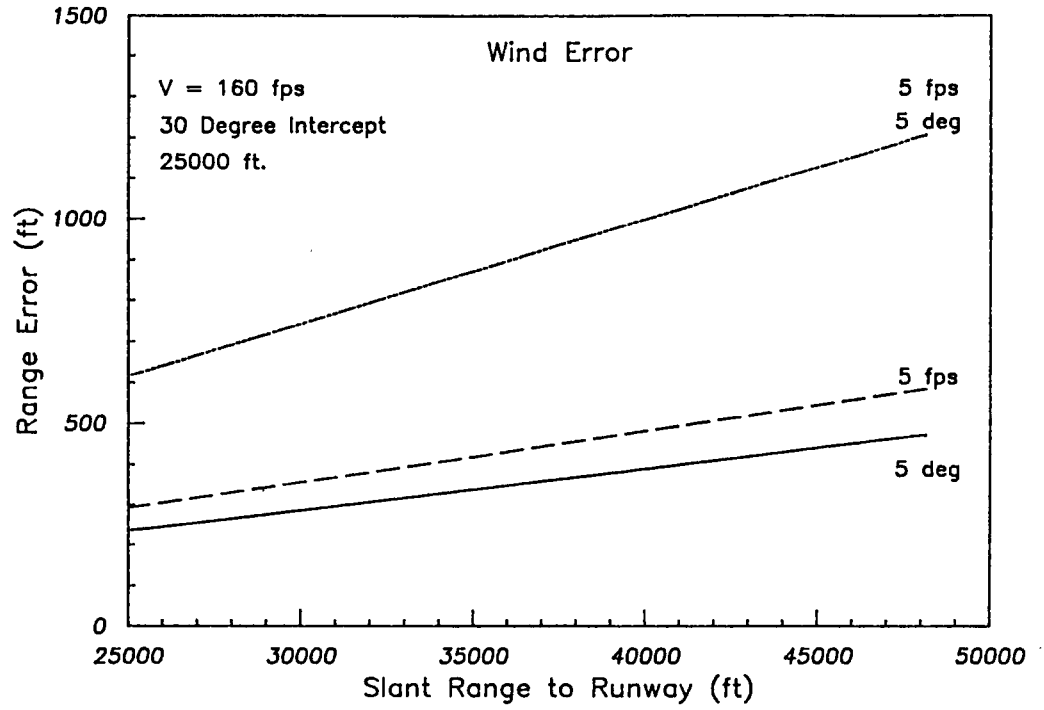

Figure B.3e: Range Estimation Error Due to Uncertainties in Wind Information. Nominal Wind: 20 fps from 135 deg.

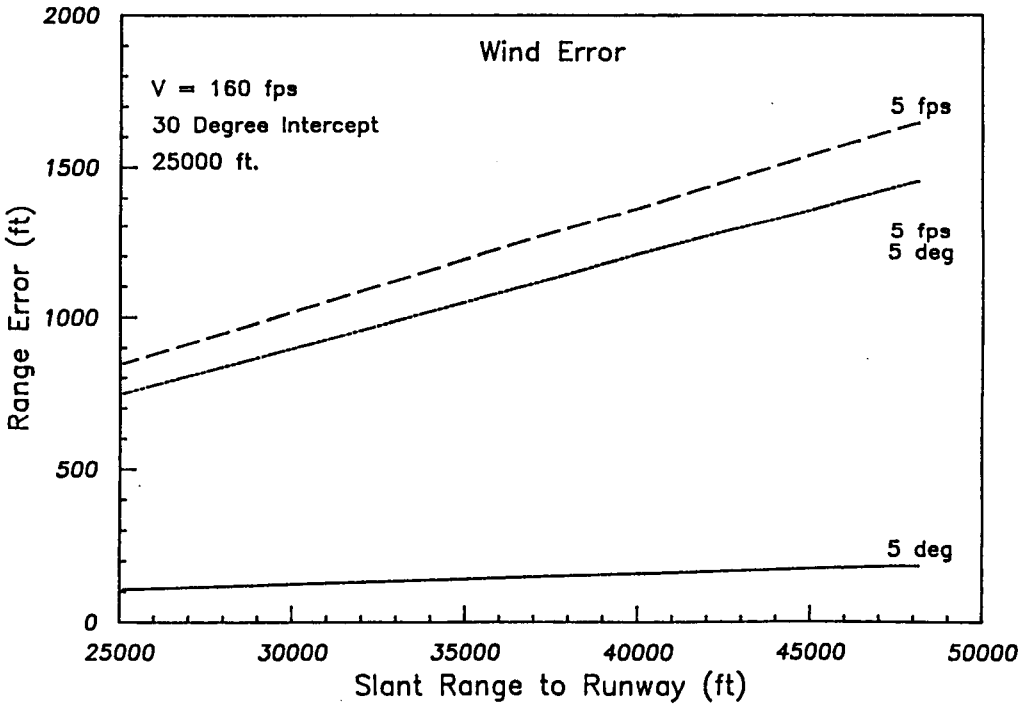

Figure B.3f: Range Estimation Error Due to Uncertainties in Wind Information. Nominal Wind: 20 fps from 225 deg.

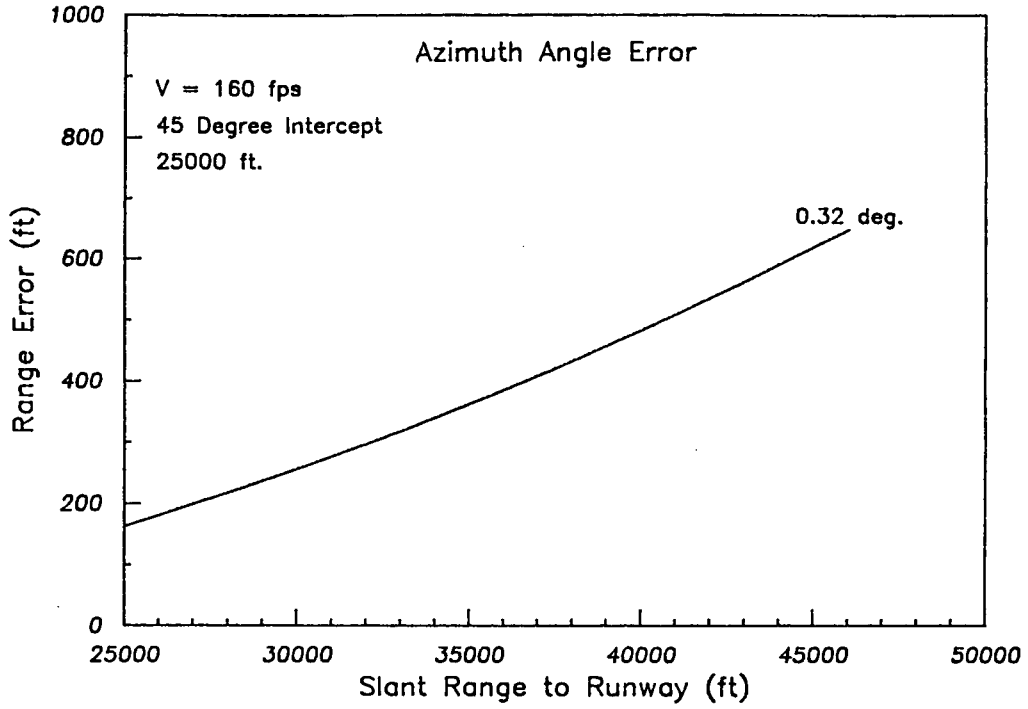

Figure B.4a: Range Estimation Error Due to Azimuth Angle Error for Constant Intercept Trajectory

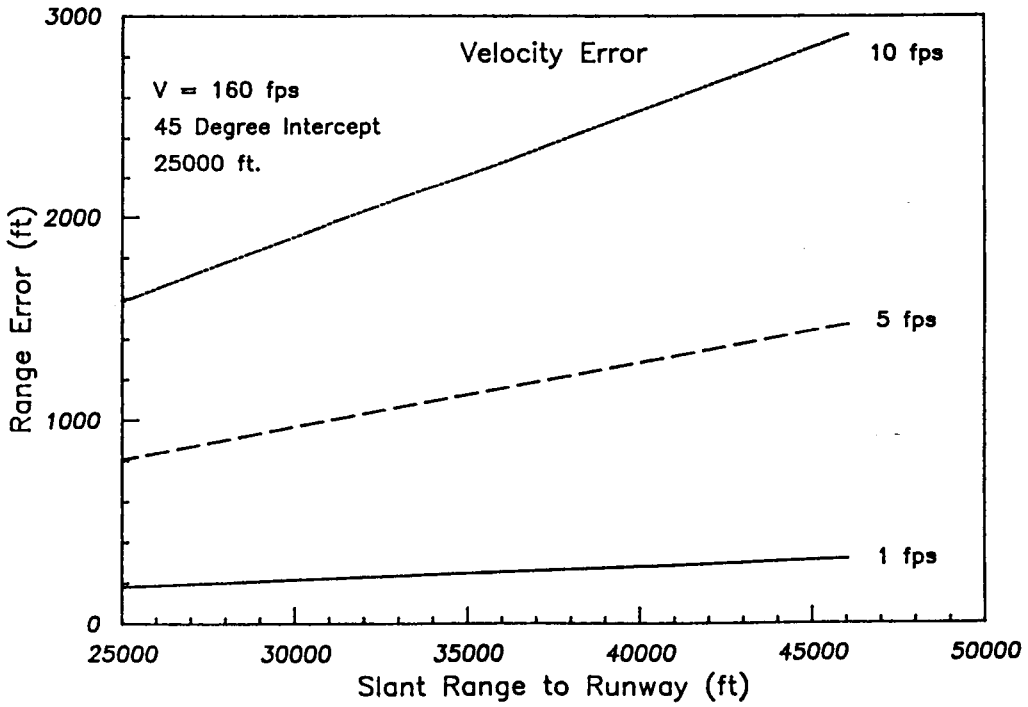

Figure B.4b: Range Estimation Error Due to Airspeed Sensor Errors

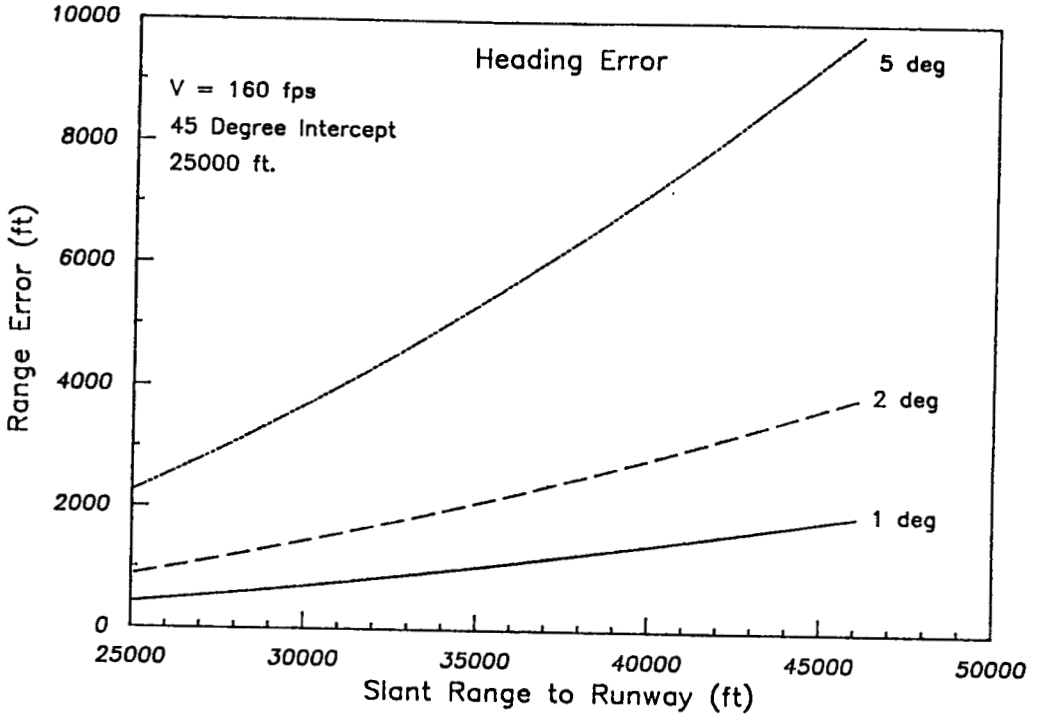

Figure B.4c: Range Estimation Error Due to Heading Sensor Error

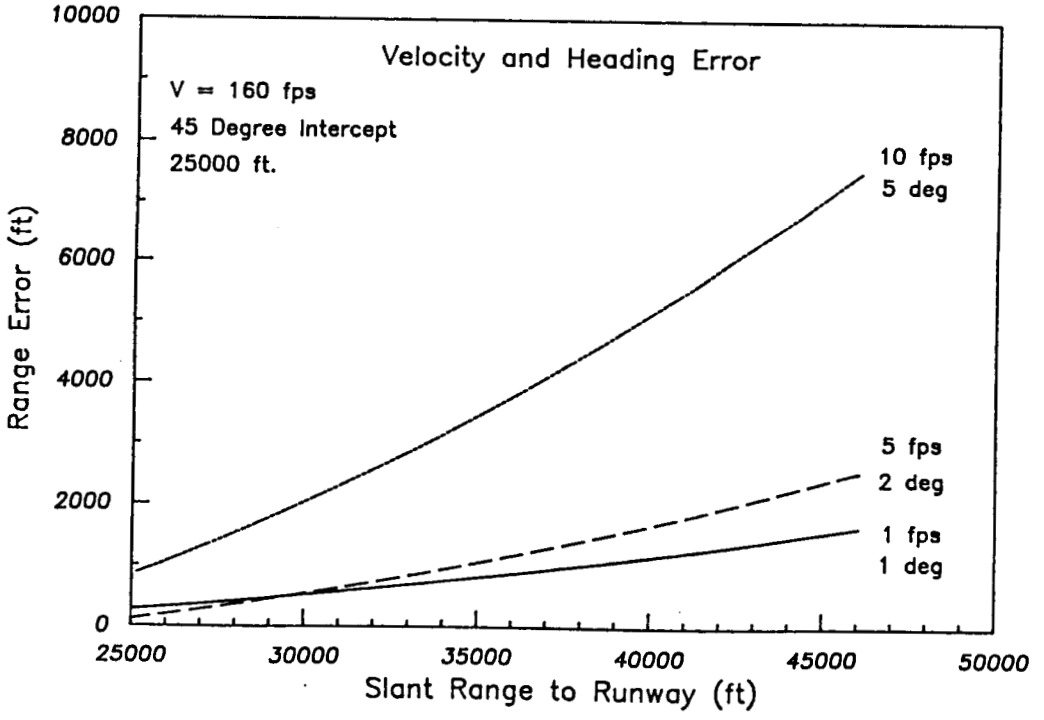

Figure B.4d: Range Estimation Error Due to Airspeed and Heading Sensor Errors

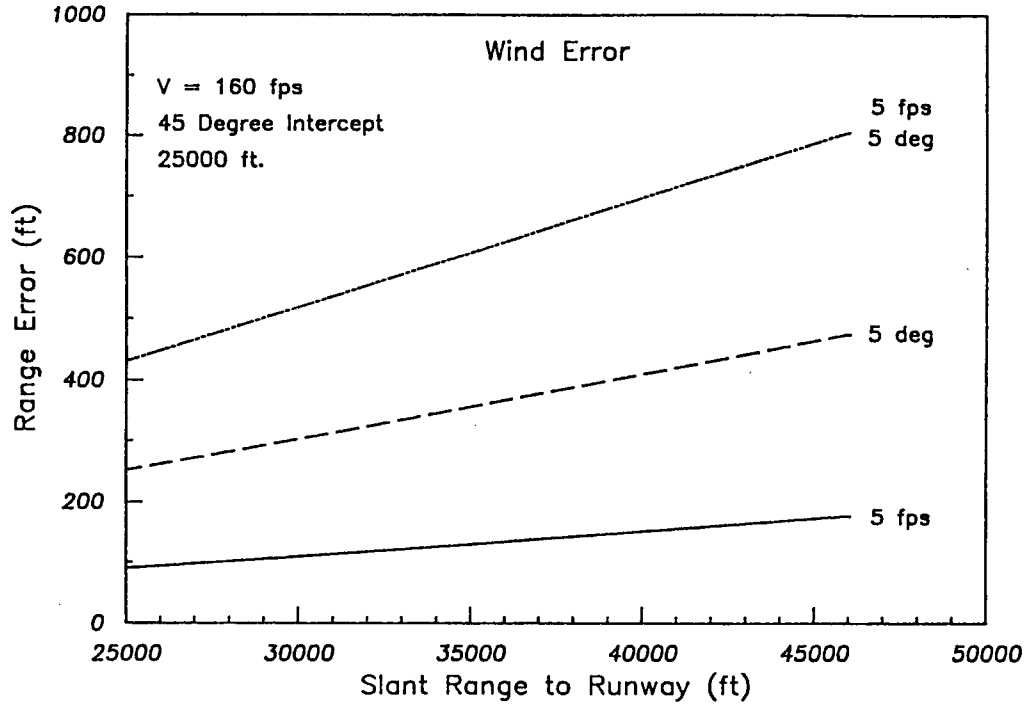

Figure B.4e: Range Estimation Error Due to Uncertainties in Wind Information. Nominal Wind: 20 fps from 135 deg.

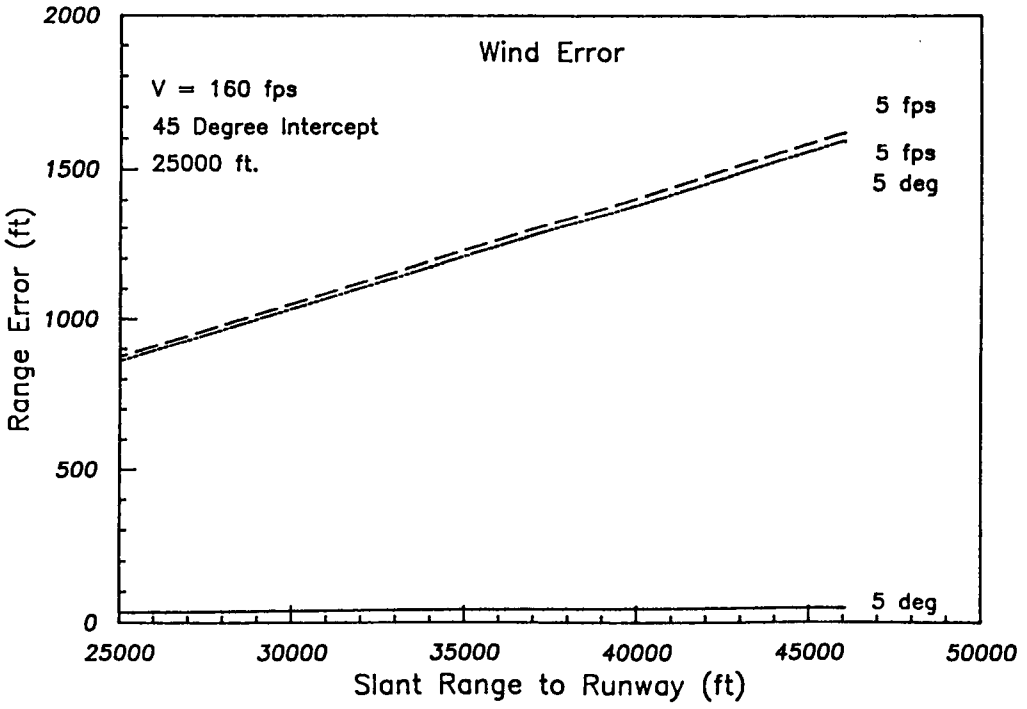

Figure B.4f: Range Estimation Error Due to Uncertainties in Wind Information. Nominal Wind: 20 fps from 225 deg.

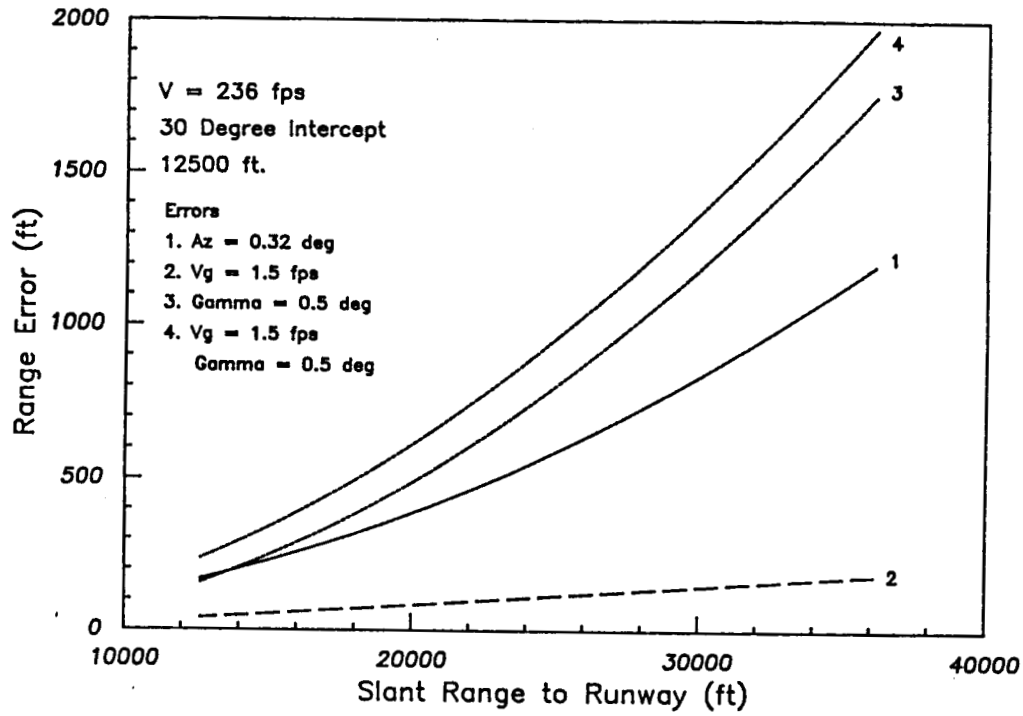

Figure B.5: Summary of Range Estimation Error for Commercial Airline Operation Using Constant 30° Intercept at 12,500 Feet

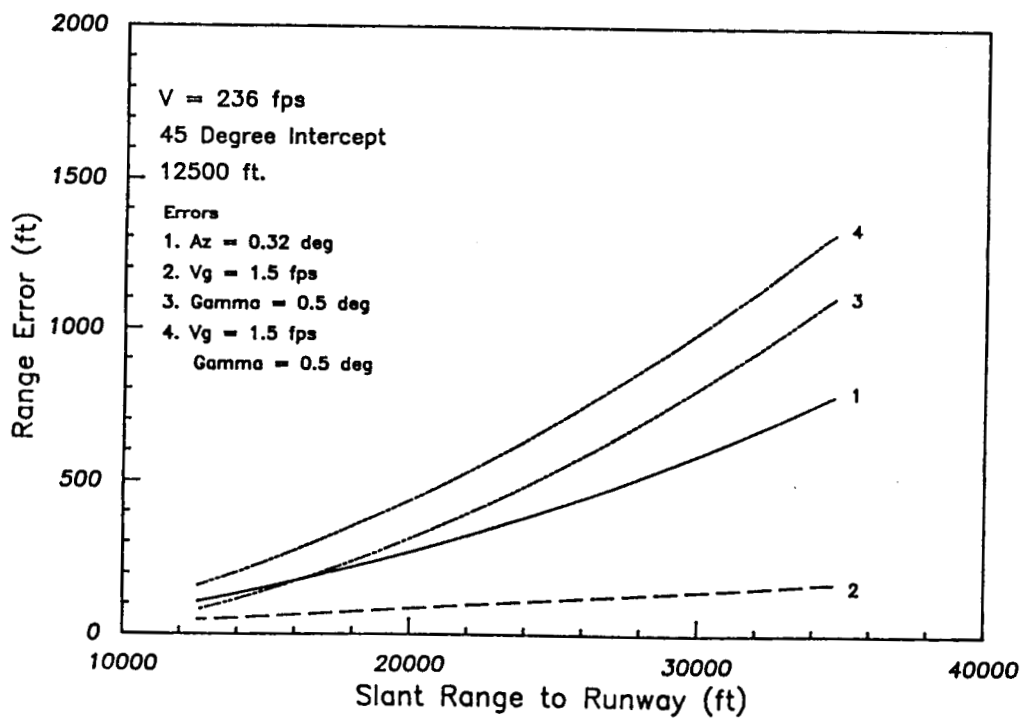

Figure B.6: Summary of Range Estimation Error for Commercial Airline Operation Using Constant 45° Intercept at 12,500 Feet

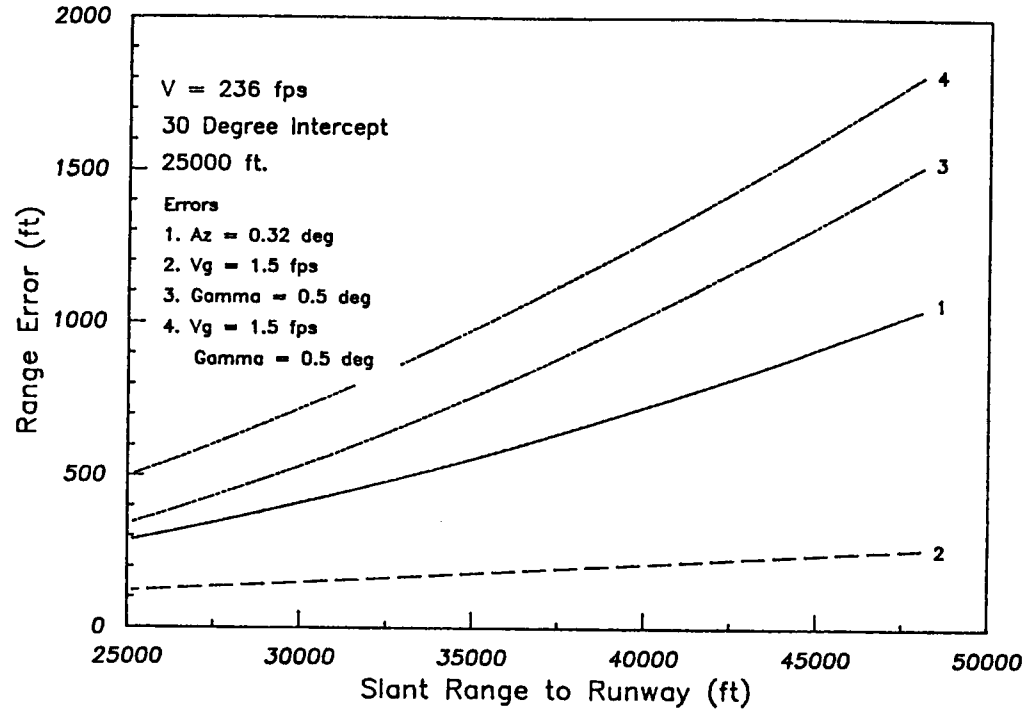

Figure B.7: Summary of Range Estimation Error for Commercial Airline Operation Using Constant 30° Intercept at 25,000 Feet

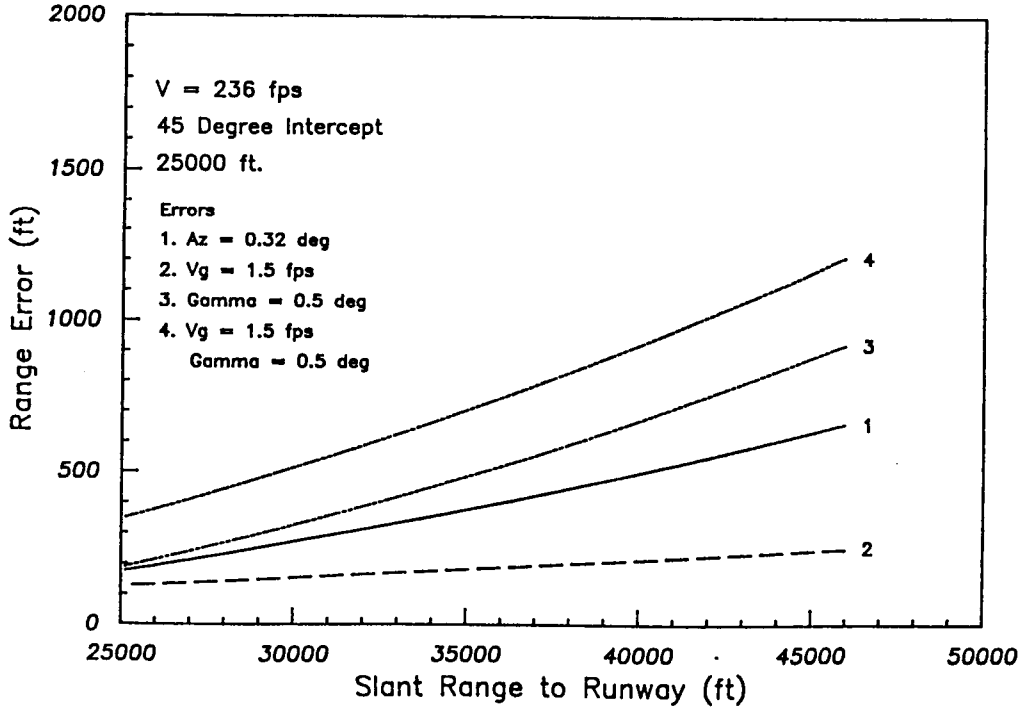

Figure B.8: Summary of Range Estimation Error for Commercial Airline Operation Using Constant 45° Intercept at 25,000 Feet

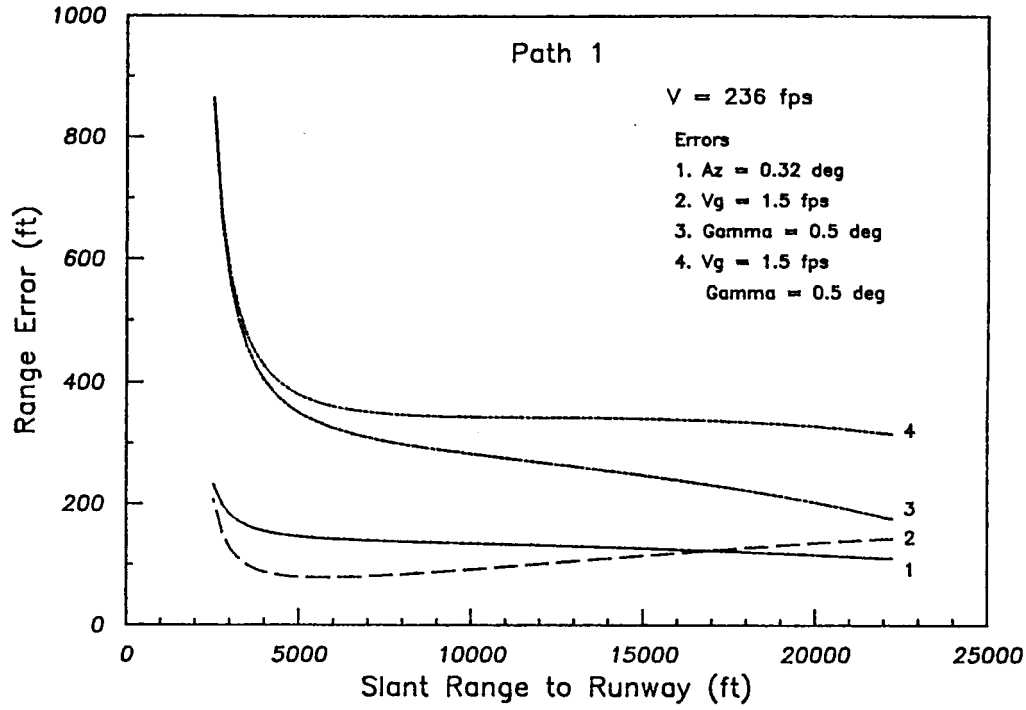

Figure B.9: Range Estimation Error for V = 236 fps, Path 1

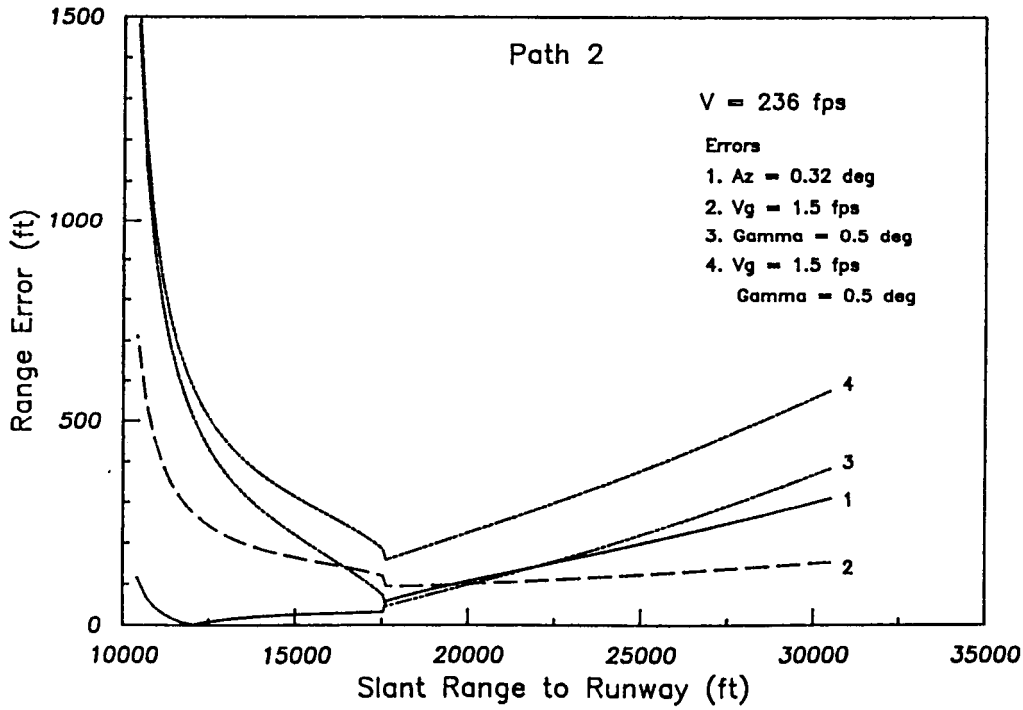

Figure B.10: Range Estimation Error for V = 236 fps, Path 2